

AS210

**R-1571**  
**ULTIMATE INTRINSIC COERCIVITY**  
**SAMARIUM-COBALT MAGNET**  
**AN EARTH-BASED FEASIBILITY STUDY FOR**  
**SPACE SHUTTLE MISSIONS**  
**FINAL REPORT**  
**JUNE 1982**  
**by**  
**D. DAS and K. KUMAR**  
**R.T. FROST and C.W. CHANG (G.E.)**

(NASA-CR-170627) ULTIMATE INTRINSIC  
COERCIVITY SAMARIUM-COBALT MAGNET. AN EARTH  
BASED FEASIBILITY STUDY FOR SPACE SHUTTLE  
MISSIONS Final Report, 1 Oct. 1979 - 30  
JUL. 1982 (Draper (Charles Stark) Lab.,

NS2-33495

HC A04  
Unclas  
GS/26 35451



**The Charles Stark Draper Laboratory, Inc.**  
Cambridge, Massachusetts 02139

## UNCLASSIFIED

SECURITY CLASSIFICATION OF THIS PAGE (When Data Entered)

REPORT DOCUMENTATION PAGE		READ INSTRUCTIONS BEFORE COMPLETING FORM
1. REPORT NUMBER R-1571	2. GOVT ACCESSION NO.	3. RECIPIENT'S CATALOG NUMBER
4. TITLE (and Subtitle)  ULTIMATE INTRINSIC-COERCIVITY, SAMARIUM-COBALT MAGNET, AN EARTH-BASED FEASIBILITY STUDY FOR SPACE SHUTTLE MISSIONS		5. TYPE OF REPORT & PERIOD COVERED  FINAL REPORT, 1 Oct 1979-30 Jun 1982
		6. PERFORMING ORG. REPORT NUMBER R-1571
7. AUTHOR(s)  D. Das and K. Kumar - CSDL R.T. Frost and C.W. Chang - General Electric Co.		8. CONTRACT OR GRANT NUMBER(s)  NAS8-33607
9. PERFORMING ORGANIZATION NAME AND ADDRESS The Charles Stark Draper Laboratory, Inc. 555 Technology Square Cambridge, MA 02139		10. PROGRAM ELEMENT, PROJECT, TASK AREA & WORK UNIT NUMBERS
11. CONTROLLING OFFICE NAME AND ADDRESS National Aeronautics and Space Administration George C. Marshall Space Flight Center Marshall Space Flight Center, Alabama 35812		12. REPORT DATE July 1982
		13. NUMBER OF PAGES
14. MONITORING AGENCY NAME & ADDRESS (if different from Controlling Office)		15. SECURITY CLASS. (of this report)  UNCLASSIFIED
		15a. DECLASSIFICATION/DOWNGRADING SCHEDULE
16. DISTRIBUTION STATEMENT (of this Report)		
17. DISTRIBUTION STATEMENT (of the abstract entered in Block 20, if different from report)		
18. SUPPLEMENTARY NOTES		
19. KEY WORDS (Continue on reverse side if necessary and identify by block number)  Magnet, Samarium-Cobalt, Coercivity, Levitation Melting, Oxygen-free Comminution, Hot Isostatic Pressing		
20. ABSTRACT (Continue on reverse side if necessary and identify by block number)  Earlier work on this contract demonstrated that reaction of electromagnetically levitated charges of elemental samarium and cobalt completely avoided crucible contamination. Subsequent work was done to reduce oxygen contamination from the helium jet necessary for temperature control of the levitated melt. This activity is described in a paper recently accepted for publication in Metallurgical Transactions.  A stainless steel glove box capable of being evacuated to low $10^{-6}$ torr pressure and refilled with ultra-pure argon has been built and installed. Necessary accessories to perform $\text{SmCo}_5$ powder preparation, compaction and subsequent encapsulation of the powder inside a hot isostatic pressing cannister have been designed, built, and		

UNCLASSIFIED

SECURITY CLASSIFICATION OF THIS PAGE (When Data Entered)

R-1571

ULTIMATE INTRINSIC-COERCIVITY  
SAMARIUM-COBALT MAGNET

AN EARTH-BASED FEASIBILITY STUDY FOR  
SPACE SHUTTLE MISSIONS

Final Report  
July 1982

By

Dilip K. Das\*, Kaplesh Kumar\*  
The Charles Stark Draper Laboratory, Inc.

and

Robert T. Frost, C. W. Chang\*\*  
Space Sciences Division  
General Electric Company

Prepared for National Aeronautics and Space Administration  
Under Contract NAS8-33607

Approved: M. S. Sapuppo  
M.S. Sapuppo, Head  
Component Development Dept.

The Charles Stark Draper Laboratory, Inc.  
Chambridge, Massachusetts 02139

\*Some of the work presented in this report was performed at the Francis Bitter National Magnet Laboratory by these authors as visiting scientists.

\*\*Presently with KBI Division, Cabot Corporation. Work was done while at General Electric Company.

#### ACKNOWLEDGEMENT

Large contributions were made by Ernest Wettstein in the design of the comminution and encapsulation chamber and its various accessories.

## TABLE OF CONTENTS

<u>Section</u>	<u>Page</u>
1 INTRODUCTION.....	1
2 OBJECTIVE.....	2
3 TASK DESCRIPTION.....	2
3.1 Alloy Melting.....	3
3.2 Powder Metallurgical Processing.....	3
4 ELECTROMAGNETIC CONTAINERLESS MELTING OF SAMARIUM-COBALT ALLOY.....	4
4.1 Introduction.....	4
4.2 Contamination Studies of Reaction System.....	5
4.2.1 Mass Spectrometer Measurements.....	5
4.2.2 Vacuum System Improvements.....	7
4.2.3 Helium Scrubber Improvements.....	7
4.2.4 Elemental Materials Used for Final Reaction Experiments.....	9
4.2.5 Final Reaction Experiments Using Pure Charges with Gas Scrubber.....	10
5 DC ARC-MELTED AND DROP-CAST $\text{SmCo}_5$ ALLOY BY AMES LABORATORY OF IOWA STATE UNIVERSITY.....	12
6 LOW OXYGEN COMMINUTION AND POWDER METALLURGY.....	13
6.1 Comminution, Compaction and Encapsulation Chamber.....	13
6.2 Modified Attritor Ball-Mill and Welding Gun.....	17
6.3 Manual Compactor.....	17
6.4 Hydrogen Comminution Apparatus.....	20

TABLE OF CONTENTS (continued)

<u>Section</u>	<u>Page</u>
7	LOW OXYGEN $\text{SmCo}_5$ FABRICATION EXPERIMENTS.....20
7.1	Attritor Ball Milling of $\text{SmCo}_5$ Powder.....22
7.2	Arc Welding Inside the Chamber.....24
7.3	$\text{SmCo}_5$ Powder Densification Using Comminution Chamber Procedure.....24
7.3.1	Metallographic Examination.....27
7.3.2	Magnetic Properties.....34
7.3.3	Oxygen Analyses.....34
8	DISCUSSION AND CONCLUSIONS.....35
	LIST OF REFERENCES.....39

## LIST OF FIGURES

<u>Figure</u>	<u>Page</u>
1	Mass spectrometer analysis of chamber impurities due to leaks and outgassing.....6
2	Vacuum glove box schematic.....15
3	The comminution and encapsulation chamber.....16
4	Attritor ball mill and the hand held welding gun inside the chamber as seen through the viewing port.....18
5	Manual compactor for loading HIP canister with highly compacted $\text{SmCo}_5$ powder.....19
6	Hydrogen comminution apparatus.....21
7	Photomicrograph of the $\text{SmCo}_5$ powder prepared by attritor ball milling in the comminution chamber.....23
8	Welded and unwelded HIP cannisters and cover - valve assemblies.....26
9	Particle size of $\text{H}_2$ comminuted $\text{SmCo}_5$ powder.....28
10	Grain size and domain structure of polished HIPed $\text{SmCo}_5$ .....30
11	Grain size and domain structure of polished HIPed $\text{SmCo}_5$ (Ames alloy).....31
12	Microstructure of commercial HIPed $\text{SmCo}_5$ .....32
13	Microstructure of Ames Alloy HIPed $\text{SmCo}_5$ .....33

## LIST OF TABLES

<u>Table</u>	<u>Page</u>
1	The ranges of weight ppm of trace elements.....12
2	Intrinsic coercivities of HIPed $\text{SmCo}_5$ materials produced from $\text{H}_2$ -comminuted powder.....34
3	Oxygen analyses of various samples.....35

ULTIMATE INTRINSIC-COERCIVITY SAMARIUM-COBALT MAGNET:  
AN EARTH-BASED FEASIBILITY STUDY FOR SPACE-SHUTTLE MISSIONS

1. INTRODUCTION

Outstanding intrinsic coercivities of 45 kOe and 70 kOe have been achieved for  $\text{SmCo}_5$  magnets at the Charles Stark Draper Laboratory (CSDL) using improved sintering processes<sup>(1)\*</sup> and arc plasma spraying.<sup>(2)</sup> Even these very high values of coercivity are only 13 and 20 percent of the theoretical maximum value of approximately 350 kOe which is the magnetic anisotropy field for pure  $\text{SmCo}_5$ . Coercivity of a magnet is indicative of its resistance to magnetization reversal when a reverse field is applied. The reversal of  $\text{SmCo}_5$  magnets at just a small fraction of their anisotropy field has been attributed to the presence of defect sites<sup>(3)</sup> where the reverse domains nucleate at lower fields and the reversal of magnetization occurs easily by domain wall propagation. Many of these defects are believed to be compositional inhomogeneities resulting from precipitation of dissolved oxygen during the cooling of the magnets from the sintering and annealing temperatures.<sup>(4-6)</sup>

---

\* Superscript numerals refer to similarly numbered references in the List of References.



## 2. OBJECTIVE

The objective of this research program was to demonstrate that it may be feasible to produce an intrinsic coercivity in an  $\text{SmCo}_5$  magnet approaching its theoretical limit of 350 kOe, as compared to the best achieved-to-date value of approximately 70 kOe at CSDL. To achieve this goal, the experimental efforts were directed towards elimination of contamination, particularly oxygen, from the finished magnet.

Generally, the sintered  $\text{SmCo}_5$  magnets contain 6000 ppm of oxygen. Using the Arc Plasma Spray (APS) fabrication process, samarium cobalt magnets can be produced with oxygen content as low as 1500 ppm. The experimental goal in this program was to produce fine particle (5  $\mu\text{m}$  or less)  $\text{SmCo}_5$  magnets with oxygen content substantially below that which has been achieved at CSDL to date (1500 ppm). It was hoped that an oxygen content below 250 ppm, and no more than 100 ppm of other contaminants, would be achieved. The purest available samarium and cobalt contain impurities other than oxygen in the neighborhood of 100 ppm. Efforts were therefore directed towards: (1) minimizing crucible and oxygen contamination during alloy melting and (2) minimizing oxygen contamination in the fabrication process of producing a fine particle magnet from the alloy.

## 3. TASK DESCRIPTION

Basically, the program was envisioned as being comprised of two main tasks:

- (1) To produce contamination-free alloys of desired composition from pure elements, samarium and cobalt.
- (2) To produce very fine powder from these alloys and to densify the powder without adding any contamination during processing, while retaining a fine-grained structure in the densified body.

### 3.1 Alloy Melting

The conventional procedure for the preparation of Sm-Co alloys is to melt elemental Co and Sm in ceramic crucibles using high frequency induction heating in an inert gas atmosphere. Because of the highly reactive nature of samarium, oxygen as well as other impurities are picked up by the alloy from both the ambient atmosphere and by reaction with the crucible walls. Two approaches were taken in this program to reduce the amount of contamination during the melting process viz, (1) containerless R.F. levitation melting in flowing helium gas at the Space Sciences Division of General Electric Company and (2) DC arc melting on a water-cooled tantalum clad copper hearth in a low oxygen quiescent argon atmosphere.

### 3.2 Powder Metallurgical Processing

Large amounts of oxygen enter the  $\text{SmCo}_5$  magnet during the powder metallurgical processes by which these magnets are fabricated. These consist of comminution and compaction in an air atmosphere followed by densification using sintering. Since the oxygen contamination in this part of processing is larger by more than an order of magnitude than what occurs in the alloy melting procedure, the program plans called for developing an entirely new approach where all the steps necessary would be performed out of contact with air, either in highly purified inert gas atmosphere or in vacuum. A chamber capable of maintaining an ultraclean oxygen-free atmosphere had to be designed and built, where comminution, compaction and encapsulation of the compacts in well outgassed iron cannisters could be performed in an oxygen-free atmosphere. The sealed cannisters could then be brought out of the chamber and the compacts densified to near theoretical density by hot isostatic pressing (HIP). The technique of densification of  $\text{SmCo}_5$  magnets by HIPing was being developed at CSDL about the time the present program was started. Since then a paper has been published in the IEEE transactions on Magnetics<sup>(7)</sup> describing the HIPing of  $\text{SmCo}_5$  magnets and is appended to this report.

#### 4. ELECTROMAGNETIC CONTAINERLESS MELTING OF SAMARIUM-COBALT ALLOY

##### 4.1 Introduction

The development of a technique for forming pure Sm-Co alloy free from the effects of crucible contamination has been described in a paper which is due for publication in Metallurgical Transactions.<sup>(8)</sup> A copy of this paper is included as Appendix 1 of this report. This technique utilizes electromagnetic levitation to avoid the use of a crucible during melting and reaction of pure elemental materials. The samarium is formed as the tightly fitting core of a cobalt cylinder, with masses being adjusted to provide proper stoichiometry for the melt. Cooling and solidification is provided by means of a jet of helium gas. In the early experiments excessive oxygen pickup from the helium coolant system was experienced. Additional work was therefore carried out to clean up the reaction chamber coolant system and to instrument measurement of the oxygen partial pressure in the chamber. A specimen of SmCo was prepared with the desired stoichiometry and with an oxygen content of 200 ppm. Although this is significantly better than that obtained earlier (600 ppm), it does not meet the 100 ppm goal which had been set as the objective required to study the improvement in magnetic properties by removal of oxygen. It was shown that the oxygen contamination was proportional to reaction time and hence may be attributed to residual oxygen in the system which is gettered due to the rapid helium flow required for temperature control of the molten sample. This report describes this work which has now been discontinued due to availability of SmCo of the desired purity from a non-commercial source.

The objectives and general techniques for levitation containerless formation of SmCo alloys have been adequately described in Appendix 1. This report describes in more detail the effort expended to reduce and instrument the oxygen partial pressure in the reaction chamber and coolant gas system and the experiments in which these improvements were shown to be partially effective.

## 4.2 Contamination Studies of Reaction System

### 4.2.1 Mass Spectrometer Measurements

A mass spectrometer, Spectromass Model 1000M, was installed in the levitation reaction chamber for the purpose of identifying contaminant species and their concentrations arising from system outgassing, leaks, and from the helium coolant system. This device allows scanning over a mass range 1-100 at selected scan rates or monitoring of selected mass peaks. Two detectors are available; an ion chamber sensitive to partial pressures between  $10^{-4}$  and  $10^{-8}$  torr, and an electron multiplier sensitive to  $10^{-10}$  torr.

The electron multiplier was used for vacuum studies to detect and reduce system leaks; the ion chamber detector was used at the higher pressures with the helium coolant system operating at low flow rates to study contamination from this system. Figure 1 shows a typical mass scan with the system under a vacuum of  $10^{-6}$  torr. Mass peaks are evident at 28 ( $N_2$ ), 32 ( $O_2$ ), in the proper ratio to represent air leaking into the system. Peaks at 14 and 16 in about the same ratio are attributed to atomic nitrogen and oxygen. The water vapor peak at 18 was observed to decrease markedly after overnight pumping, indicating this water was probably absorbed when the system was open. The OH peak at 17 is also evident. Measurements using the electron multiplier showed additional weak peaks due to hydrocarbons, but these were generally weaker by two orders of magnitude than the main peaks due to air.

ORIGINAL RECORDS  
OF POOR QUALITY

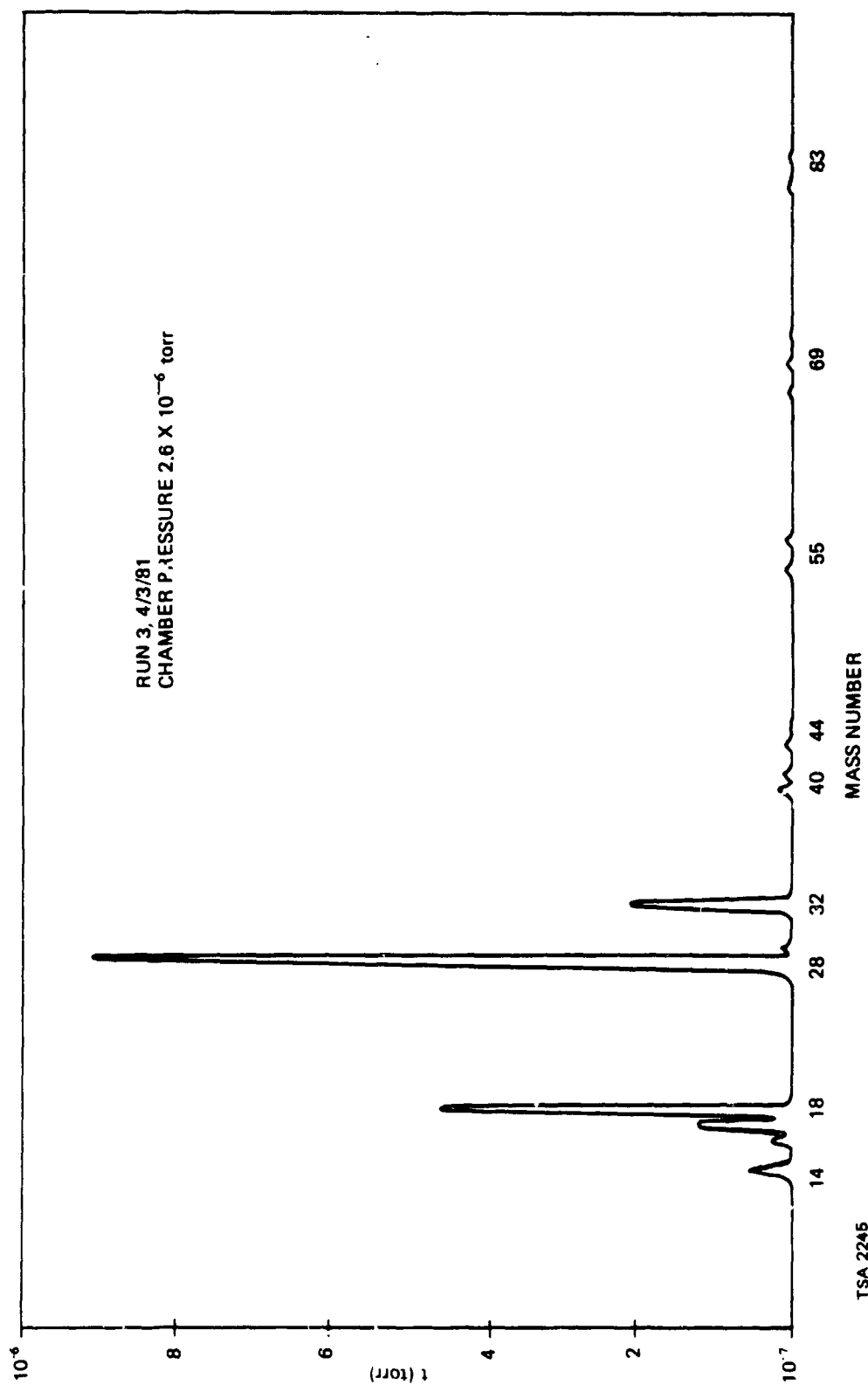


Figure 1. Mass spectrometer analysis of chamber impurities due to leaks and outgassing.

#### 4.2.2 Vacuum System Improvements

Since the mass spectrometer can be utilized as a very effective leak detector, it was used to localize and reduce several system leaks. Leaks were found and reduced at the following system locations:

Helium, -ye valve.

This leak was intermittent, and hence had been previously unidentified.

Chamber pressure gauge (for measuring helium pressure).

After correcting these leaks, it was found possible to pump the system to the mid- $10^{-7}$  torr range. The leak-up rate of the chamber was measured and found to be about  $1.5 \times 10^{-7}$  gm of  $N_2$   $\text{sec}^{-1}$ . Although this leak rate is eliminated with the system under helium pressure slightly exceeding one atmosphere gauge pressure, it is effective during the interval between vacuum purging of the chamber and admission of helium to its full final pressure. The time interval for admission of helium is limited by the helium scrubber, in which the temperature of the scrubber cannot be allowed to drop excessively by helium flow; otherwise its effectiveness for gettering oxygen is reduced.

#### 4.2.3 Helium Scrubber Improvements

An inert gas scrubbing system was available with copper screen getter and a heater capable of maintaining the copper screens at  $500^\circ\text{C}$ . To improve the gettering action, particularly with higher gas flows where the getter temperature might be reduced, titanium chips were procured and used to replace the copper. Titanium chips were installed in the getter tube of length 14 inches and diameter 1-1/4 inch. These chips are effective down to temperatures of  $350^\circ\text{C}$ , according to their manufacturer (General Electric Nuclear Division). Mass spectrometer

measurements with low rates of helium entering the chamber with the getter heated showed significant reductions in the water vapor peak but not total elimination. This was interpreted as due to outgassing of absorbed water vapor in the walls of the unbaked reaction chamber.

To allow pressurization of the processing chamber, which is normally used as a vacuum chamber, tie-down straps were added capable of maintaining the seal gasket under compression with a fraction of a pound per square inch gage pressure in the chamber. Venting of the chamber during the high temperature reaction of samarium-cobalt was necessary because of the relatively high volume flow of helium in the jet required for temperature control of the reacting mass and the inability of the processing chamber to withstand high internal pressures. It was also considered beneficial to flush any oxygen and water vapor that might be evolved from secondary heating of the processing chamber walls and internal parts.

In order to measure the relative contributions to chamber gas impurities arising from the helium coolant gas system and outgassing and leaks from the chamber, a number of experiments were run at low pressure where the rate of admission of helium was varied and the partial pressures of helium, nitrogen, oxygen and water vapor were measured. At the lowest flow rates, the impurity/helium ratio is determined by the outgassing and leak rates; at the higher flow rates and higher chamber pressures, the helium impurity content will ultimately dominate. Inconsistent results were obtained. Measurements of partial pressure of helium as recorded by the mass spectrometer versus the pressure as indicated by the system ion gauge indicated a pronounced nonlinearity. It was found that the indicated helium partial pressure actually went through a maximum at an ion gauge indicated pressure of  $2 \times 10^{-4}$  torr due to scattering in the mass quadrupole, which was in the range where accurate measurements were necessary to separate the outgassing and helium impurity source contributions. For this reason, unique separation of these two source contributions was not possible with the available instrumentation.

An oxygen partial pressure analyzer of the hot filament type was obtained and utilized. This instrument, manufactured by Air Products and Chemicals Corporation, is sensitive to an oxygen partial pressure of a few parts per million but has a time constant at this low pressure measured in minutes. Tests were made of the gas directly out of the helium cylinders after passing through the activated gas scrubber. Oxygen contents a few parts per million above the analyzer threshold, were measured for the tank gas, but with the scrubber in operation, the analyzer indicated reduced oxygen partial pressures.

Intermittent difficulties were encountered with higher oxygen levels and it was discovered that these appeared associated with the vent valve. It was suspected that, at the low internal oxygen pressures, backstreaming of atmospheric oxygen through the vent valve could occur against the relatively low velocity short column of exiting helium. For this reason, a vent tube of several feet length was added to the vent valve, since calculations showed that backstreaming would not occur for this situation. In one of the early runs, overheating of the samarium cobalt melt caused visible vapor clouds of samarium in the chamber. This material was seen exiting the vent valve and was believed to be a health hazard, no hood being available in the vicinity of the reaction chamber. For this reason the vent exit pipe was introduced into the forepump manifold for subsequent runs. Because of the relatively low ( $< 1$  torr) forepump pressure and the high aspect ratio of the vent tube, backstreaming was not believed to occur.

#### 4.2.4 Elemental Materials Used for Final Reaction Experiments

Elemental samarium and cobalt of improved purity was purchased for the final reaction experiments in the improved reaction chamber system with refurbished gas scrubber. One-half inch diameter samarium rod produced by vacuum zone refining was purchased through United Mineral and Chemical Corporation from a United Kingdom supplier. The material was advertised as 99.99 percent pure. Three-eighths inch diameter cobalt rod was purchased from Materials Research Corporation.



This material was believed to contain less than 0.01% oxygen by weight. A inert gas fusion analysis subcontracted by CSDL gave the following results for oxygen:

Sm: 1 ppm O<sub>2</sub>  
Co: 27 ppm O<sub>2</sub>.

The samarium was received from the vendor sealed in a glass ampule and was handled in an inert gas environment except for the brief time required for machining to form the levitation charge. It is interesting that the results obtained by CSDL are considerably better than the oxygen contents advertised by the suppliers. The chemical analyst, however, is understood to have been using a method considerable better than earlier conventional methods.

#### 4.2.5 Final Reaction Experiments Using Pure Charges with Gas Scrubber

The limited diameter of the available pure cobalt required formation of somewhat smaller charges of pure materials than had been used previously (4.8 vs. 6.2 gm). The samarium was machined into the form of a right cylinder which was tightly fitted into a cylindric concentric mass of cobalt with pressed end caps. Small grooves and end cap holes were provided to vent samarium vapor which would form before reacting to Sm-Co. This technique proved successful in preventing ballooning or expansion of the charge during reaction.

Measurement of oxygen partial pressure in the helium coolant exiting the chamber with the cooling gas jet operating before heating of the specimen indicated a value less than a few parts per million, the lower limit detectable with the hot wire partial pressure analyzer.

Following the chemical reaction of the heated levitation charges, the oxygen partial pressure in the exiting helium coolant was again found to be less than a few parts per million. It should be noted, however, that because the time constant for detection of even higher

levels is longer than the reaction time of approximately one minute, a moderate rise in oxygen level might have occurred due to outgassing from heating of the chamber and internal components during the reaction of the Sm-Co.

The paper in Appendix 1 describes in detail the results obtained by crucibleless reaction of the samarium and cobalt. Considerable improvement in oxygen level was obtained over previous runs (0.02 percent vs. 0.06 percent). It is of interest to compare this lower figure to the amounts which could have been contributed by impurities in the starting elemental materials and by the helium coolant gas.

For stoichiometric  $\text{SmCo}_5$ , the cobalt contributes a fraction 0.66 of the total mass. A weight fraction 27 ppm  $\text{O}_2$  in the starting cobalt would thus contribute only 18 ppm  $\text{O}_2$  to the weight of  $\text{SmCo}_5$ . This is only about 0.002 w/o. Likewise the contribution of oxygen from the starting samarium would be negligible compared to the 0.02 w/o found in the reacted mass.

The total oxygen content found in the final reacted 5 gm mass of SmCo was  $2 \cdot 10^{-4} \times 5 = 1$  mg. The volume occupied by this amount of oxygen at atmospheric pressure would be  $(1/32) \cdot 10^{-3} \cdot 22$  liters =  $2/3 \text{ cm}^3$ . If initially present as impurity in the helium filling the 60 liter reaction chamber, the oxygen partial pressure would be about 10 ppm. If this oxygen in the specimen were all derived from chamber oxygen, this would imply that gettering of oxygen was not significantly inhibited by diffusion. Since the helium coolant flow during the reaction was sufficient to replace the chamber helium, this would imply that the hot samarium cobalt specimen acted as an almost perfect getter for the oxygen impurity impinging from the small jet directed from close range. This would imply in turn that repeating the experiment in a microgravity would be of interest where the helium jet would not be necessary for temperature control since the electromagnetic heating would not be determined by the strong fields necessary for levitation.

ORIGINAL 10-11-60  
OF POOR QUALITY

5. DC ARC-MELTED AND DROP-CAST  $\text{SmCo}_5$  ALLOY BY AMES LABORATORY OF IOWA STATE UNIVERSITY

A 100-gram  $\text{SmCo}_5$  alloy ingot has been obtained from the Ames Laboratory, prepared specifically for our program on a special purchase order. The samarium used for the alloy was of the highest purity obtainable, prepared and purified at the Ames Laboratory. High-purity cobalt purchased commercially was also further purified at their facilities. The alloy of these two elements in the desired composition was arc-melted in a quiescent atmosphere of purified argon, on a water-cooled-tantalum-clad, copper hearth. After repeated melting to produce homogeneity, the melt was drop-cast into a cold copper mold. The alloy ingot after being received at CSDL was thoroughly analyzed to determine its quality. Some samples picked from random locations on the ingot have been analyzed for oxygen and were found to contain an average of 70 ppm oxygen by weight. In comparison, the commercial alloys contain between 200 and 400 ppm oxygen, and the recent R.F. containerless melted alloy has shown the value of 200 ppm.

Several samples of both the Ames Laboratory  $\text{SmCo}_5$  alloy and a commercial alloy of the same chemical composition were sent out for analysis of trace elements by carbon-arc optical emission spectrography. The results of the analysis are shown in Table 1.

Table 1. The ranges of weight ppm of trace elements.

Elements +		Al	Ca	Mg	Fe	Mn	Ni	Cu	Ag	Ta
Ames Alloy	Low	49	110	10	17	ND*	ND	110	35	ND
	High	180	168	34	79	20	120	120	85	
Commercial Alloy	Low	300	340	44	450	195	1160	370	40	ND
	High	3000	2300	3300	950	300	2400	510	410	

\*ND - not detectable, which usually indicates the amount as less than 10 ppm.

The large variations seen in amounts of various elements from sample to sample of the same alloys raise some doubts about the precision of the technique for quantitative chemical analysis. The variations in the Ames alloy samples were smaller, indicating a higher degree of homogeneity than in the commercial alloy. Nevertheless, it is quite apparent that the total impurity content of the Ames alloy is about an order of magnitude less than in the commercial alloy. This result was expected, since the starting materials used in the preparation of the Ames  $\text{SmCo}_5$  alloy were of the highest purity obtainable.

Based on all the analysis carried out, the  $\text{SmCo}_5$  alloy prepared at the Ames Laboratory was considered best suited for the fabrication of high purity magnets in the present program. Therefore four more 100-gram alloy ingots were purchased from the Ames Laboratory.

## 6. LOW OXYGEN COMMINUTION AND POWDER METALLURGY

### 6.1 Comminution, Compaction and Encapsulation Chamber

A large amount of oxygen (as much as 6000 ppm) is absorbed by the alloy powder of average 10  $\mu\text{m}$  particle size upon exposure to air. In the standard procedure, comminution and all powder handling is performed in air, until the green compacts enter the sintering furnace. Under very carefully controlled conditions, sintering can be performed without any large increase in oxygen content. At Draper Laboratory we have developed HIP for  $\text{SmCo}_5$  magnets, which is superior to sintering in lowering oxygen pickup during the densification of the powder compact.

The major problems that need to be solved are the preparation of powder from the  $\text{SmCo}_5$  alloy without exposure to any oxygen source and introduction of the powder compact into a well-outgassed HIP cannister, followed by evacuation and sealing of the cannister. All of the above steps can be performed inside a chamber filled with ultra-pure noble gas. Such a chamber was designed at CSDL and was built at a local vendor's facility. A schematic sketch of the entire system is shown in Figure 2.

The chamber, built of stainless steel with polished walls and stainless steel plumbing, is capable of being evacuated and baked out to reach a low  $10^{-6}$  torr pressure. Besides the main chamber where all the powder preparation and handling are performed using gloves, there are two attached auxiliary chambers, one for powder drying and the other an entry port. After evacuation the chamber is filled with getter-furnace purified-argon to atmospheric pressure. The final comminution of the powder is carried out inside the chamber, dried in the attached desiccator, loaded into the HIP cannister and compacted at 4000 lb/in<sup>2</sup>. The HIP cannister is then sealed by welding before being brought out for HIPing.

The CSDL designed comminution chamber was fabricated with all necessary stainless steel plumbing, valves, ports, and pumps. It was leak checked to less than  $10^{-9}$  std cm<sup>3</sup>/sec at the vendor's shop and delivered to CSDL by the end of December 1981. Figure 3 shows the chamber as installed at CSDL. The pumps are located under the chamber, and are partially visible. The evacuable glove port covers are in place. At the bottom right hand corner the electrical control panel is seen. A 500 rpm motorized magnetically driven shaft is located at the top of the chamber, which rotates the pedal of an attritor ball mill. The double door cylindrical entry port is seen attached on the right of the main chamber. The powder drying chamber is barely visible on the left-hand side. Not seen in the photograph are (1) a Hobart welding power supply capable of producing 200 amps at 40 volts and (2) a gas purifying system - Centorr Gettering Furnace - with gas purification

ORIGINAL PAGE IS  
OF POOR QUALITY

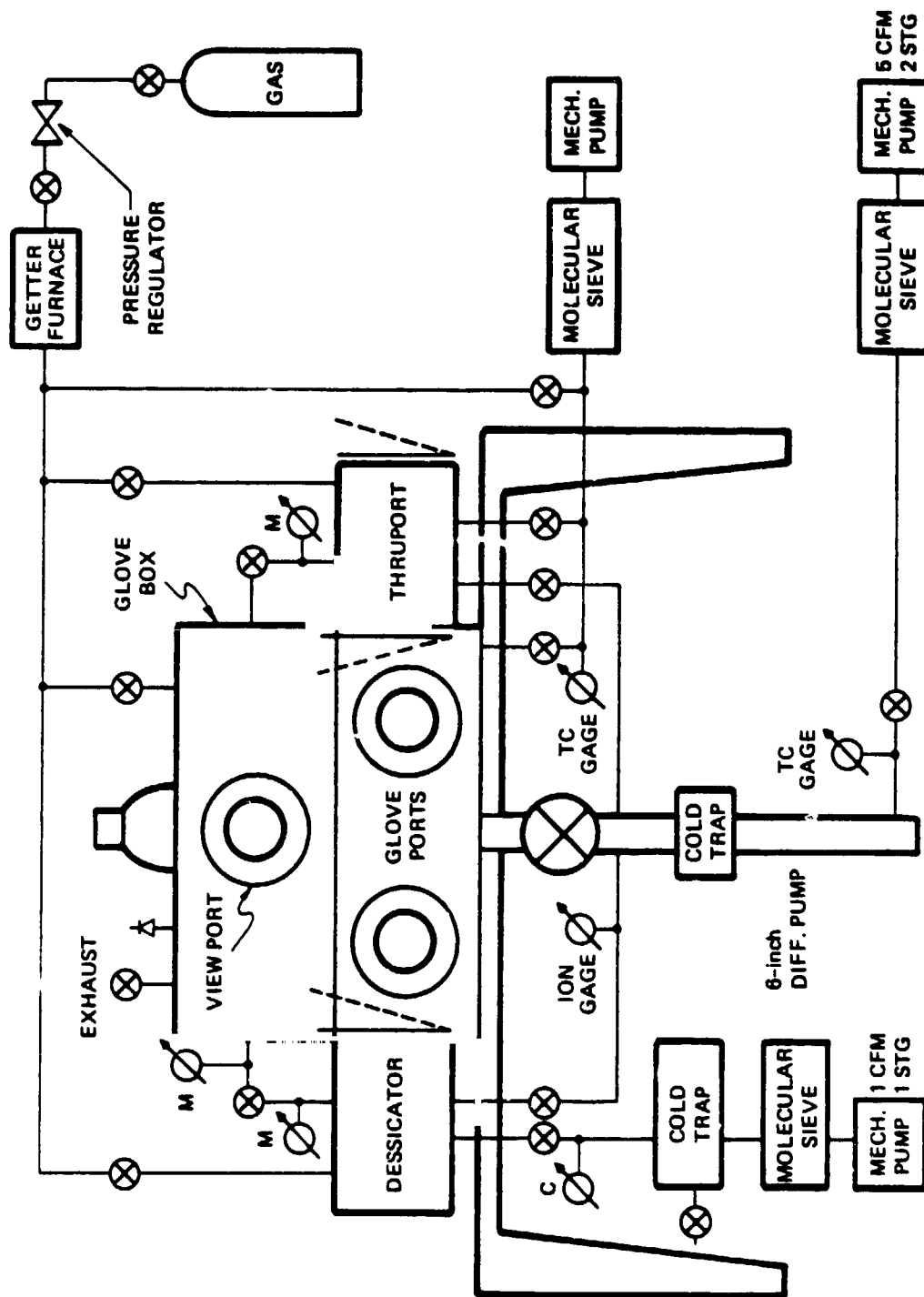


Figure 2. Vacuum glove box schematic.

TSA 2122

ORIGINAL PAGE  
BLACK AND WHITE PHOTOGRAPH

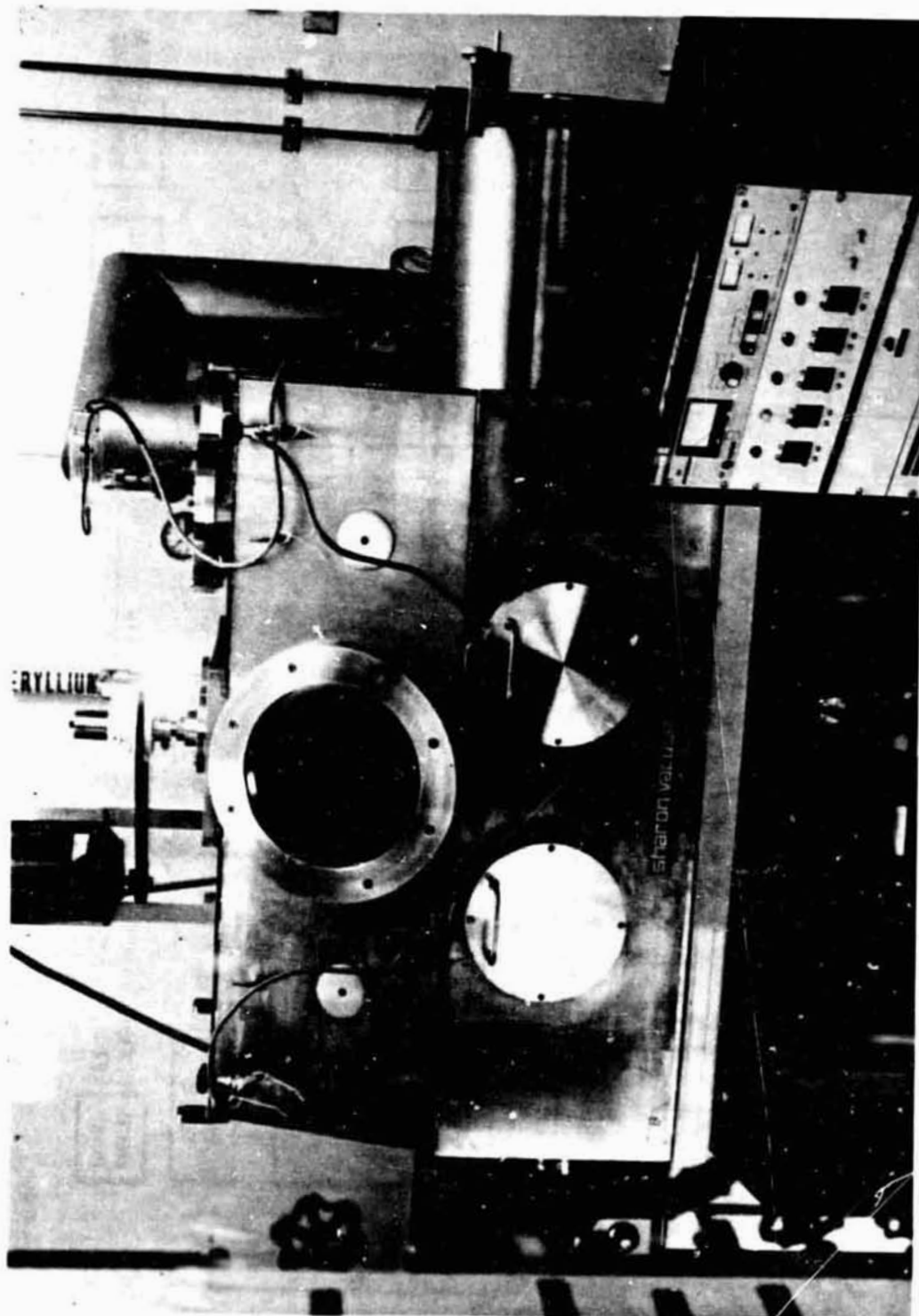


Figure 3. The comminution and encapsulation chamber.

TSA 1246

capability of less than  $10^{-6}$  ppm at a flow rate of 40 liters/minute. The welding current is brought into the chamber through a heavy duty electrical feedthrough and the purified argon gas through valved copper pipe, located in the rear wall of the chamber.

#### 6.2 Modified Attritor Ball-Mill and Welding Gun

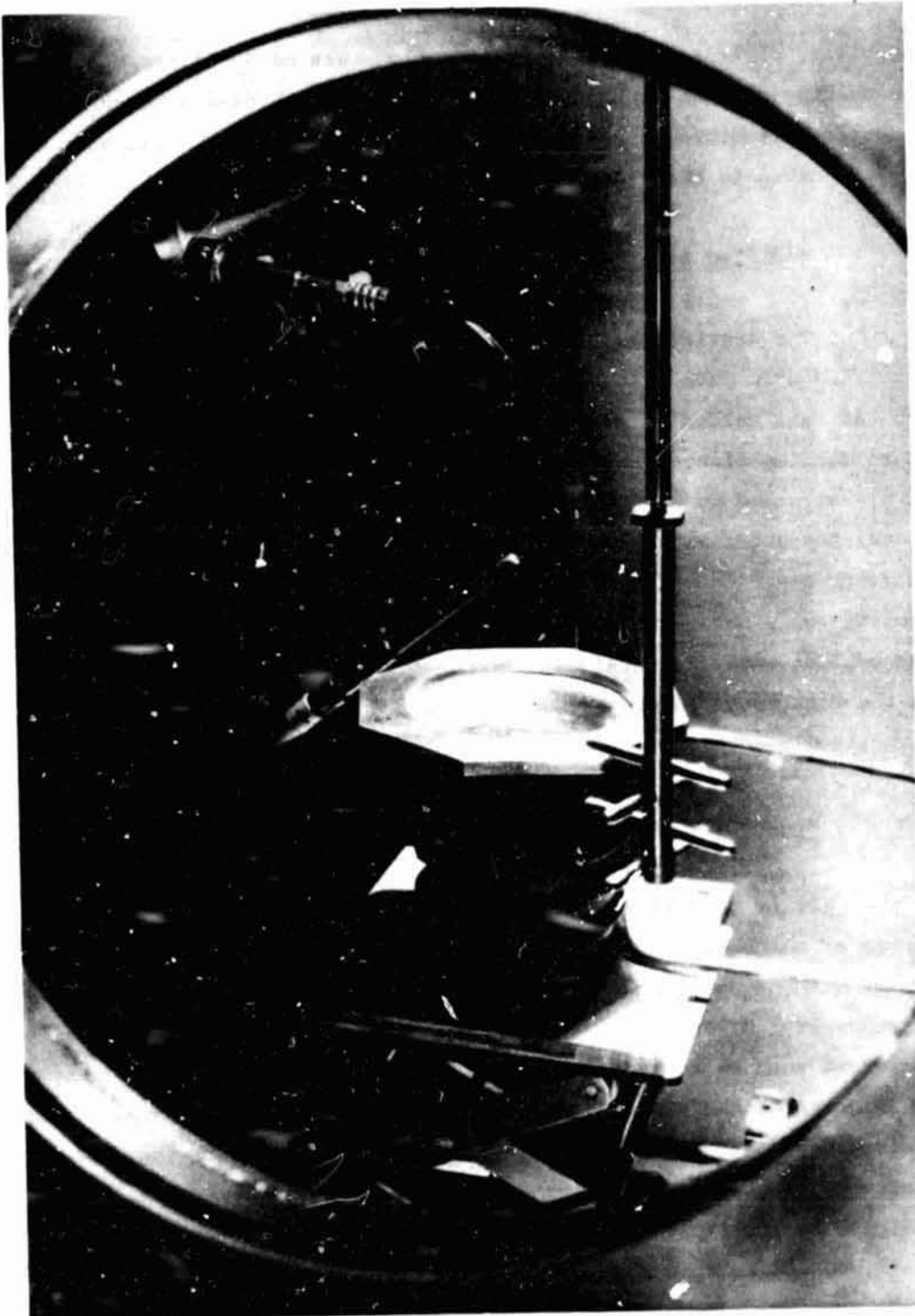
The attritor ball-mill shown in Figure 4 is a modification of a purchased unit made suitable for use inside the chamber. The attritor can had been welded to a stainless steel base plate which can be clamped on to the top plate of a laboratory jack. The base of the jack can be firmly attached to the floor of the chamber using four bolts. At that state, the shaft with attritor pedal is aligned with the axis of the attritor can. The jack is then adjusted for the proper height. Water cooling coils have been brazed on the outside wall of the attritor can and cooling water is furnished through metal bellows tubes. Also seen in the background is the arc welding gun connected to the heavy duty electrical feedthrough.

#### 6.3 Manual Compactor

Prior to HIPing, the powder is generally compacted by any of a number of means to about 65 to 70 percent of theoretical density. The tap density of  $\text{SmCo}_5$  powder is about 30 percent, which is not conducive to successful HIPing.  $\text{SmCo}_5$  powder prepared inside the chamber therefore must be compacted to a reasonable high density prior to sealing inside the HIP cannister (while still inside the chamber). The easiest way to achieve that objective would be to compact the powder directly into the HIP cannister. A manual compactor was therefore designed and built as shown in Figure 5. The entire fixture is built of stainless steel, with the top plate at a height of 12 inches from the base. The top and bottom plates are rigidly parallel to each other by means of four 1-inch diameter rods. The middle plate slides up and down the corner posts on shrink fitted nylon bushings into the holes on the plate. Motion in the vertical direction is provided by the hand crank



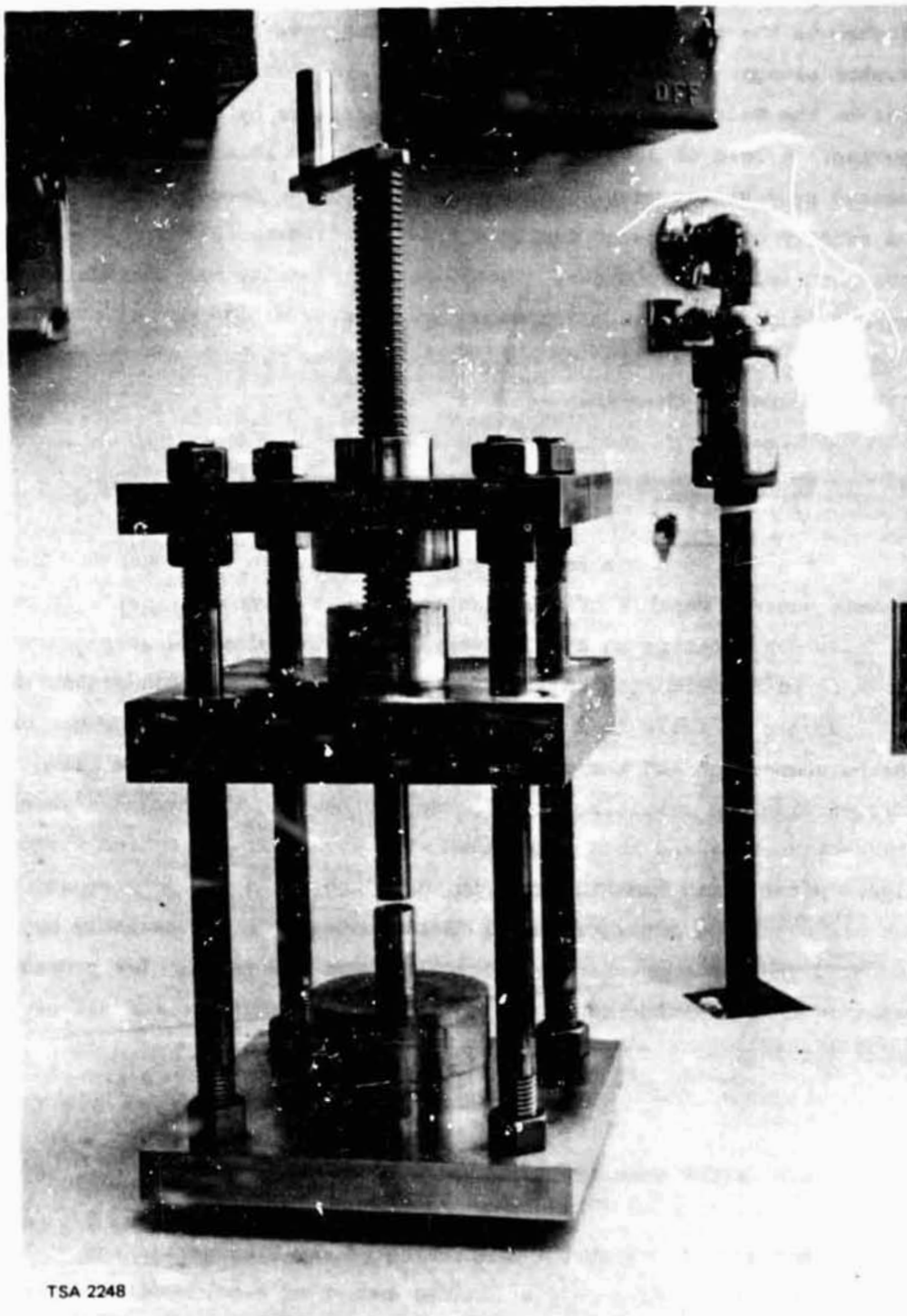
ORIGINAL PAGE  
BLACK AND WHITE PHOTOGRAPH



TSA 2247

Figure 4. Attritor ball mill and the hand held welding gun inside the chamber as seen thru the viewing port.

ORIGINAL PAGE  
BLACK AND WHITE PHOTOGRAPH



TSA 2248

Figure 5. Manual compactor for loading HIP canister with highly compacted  $\text{SmCo}_5$  powder.

attached to the threaded 1-inch diameter ACME rod. The 3/4-inch-diameter plunger attached to the sliding plate provides the compacting force on the  $\text{SmCo}_5$  powder inside the HIP cannister by means of hand cranking. A load of 2000 lbs was easily produced in this device as measured by a Dillon gage. Using this force  $\text{SmCo}_5$  powder was compacted to a density of 55 percent inside a 3/4-inch diameter HIP cannister shown just below the plunger. The 55 percent density was considered adequate to proceed with HIP processing. The assembled manual compactor could be easily moved into or out of the chamber through the entry port of the comminution chamber.

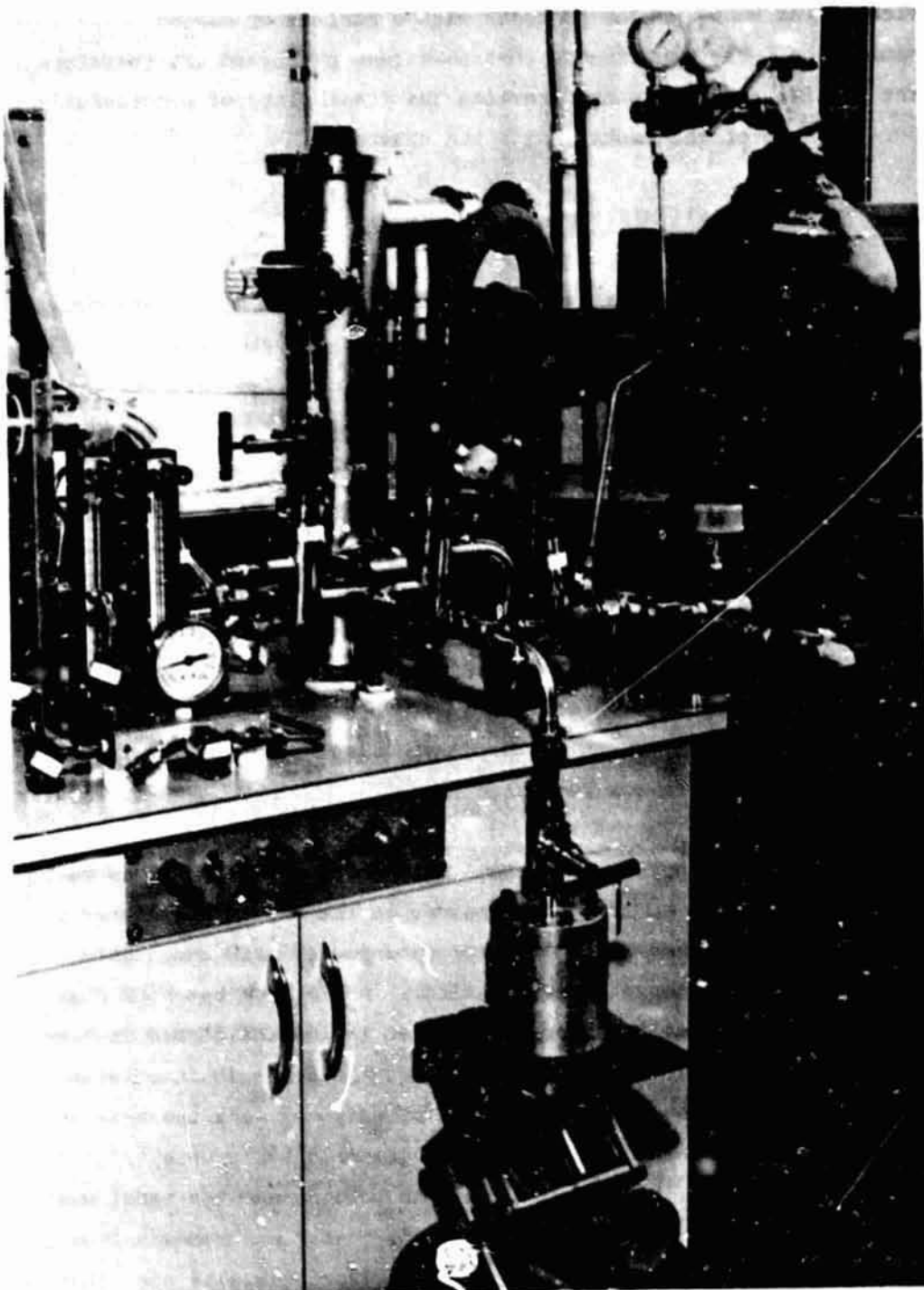
#### 6.4 Hydrogen Comminution Apparatus

The hydrogen comminution apparatus is shown in Figure 6. The pressure vessel, capable of withstanding many thousands of psi's is on the foreground resting on a laboratory jack. The plumbing arrangement allows it to be evacuated to low  $10^{-6}$  torr pressure and then pressurized with hydrogen directly from a hydrogen pressure cylinder. Hydrogen can then be pumped out and the pressure vessel baked out to remove all hydrogen from the resulting  $\text{SmCo}_5$  powder by heating the pressure vessel with heating tape and then backfilled with argon through a high vacuum valve. After argon backfilling, the valve above the pressure vessel is shut tight and the pressure vessel disconnected from the assembly by loosening the VCO connector nut directly above the valve. The pressure vessel is then transferred to the comminution chamber for removal of powder for further processing in pure argon.

#### 7. LOW OXYGEN $\text{SmCo}_5$ FABRICATION EXPERIMENTS

Because of the abrupt shortening of the time period and reduction of the funding only a limited amount of experiments could be performed in order to demonstrate the potential of the facilities for

ORIGINAL PAGE  
BLACK AND WHITE PHOTOGRAPH



TSA 2249

Figure 6. Hydrogen comminution apparatus.

fabrication of  $\text{SmCo}_5$  powder products with a minimal of oxygen contamination. The experiments that have been performed are therefore of the preliminary nature to determine the feasibility of successfully performing some of the tasks inside the chamber.

#### 7.1 Attritor Ball Milling of $\text{SmCo}_5$ Powder

In the conventional sintering process for  $\text{SmCo}_5$  magnets the particle size of the powder used is on the average between 5 and 10  $\mu\text{m}$ , which is produced by attritor ball milling. The feed for the attritor ball mill is usually around 150  $\mu\text{m}$ , which is produced by dry grinding in a double disc pulverizer. By careful processing, this powder can be produced with an oxygen content as low as about 350 to 400 ppm, starting with a good quality commercial  $\text{SmCo}_5$  alloy containing about 150 ppm of oxygen. The sinter-grade powder (5 to 10  $\mu\text{m}$ ) however contains on the average about 6000 ppm of oxygen, because the final grinding, drying of the powder and handling, etc., are all done in air. The plan for this program was therefore to perform all the tasks in the oxygen free atmosphere of the comminution chamber after the alloy was reduced to the attritor feed size powder.

The preliminary attritor ball milling in the chamber was to determine whether the modified arrangement of the mill necessitated by being inside the chamber would still produce powder size comparable to that produced by the conventional attritor. A 200 gram batch of disc ground  $\text{SmCo}_5$  powder was attritor ball milled inside the closed chamber in air atmosphere. Except for the long magnetic drive shaft rotating the attritor pedal, the other conditions of grinding were the same as when it is operated in air. As usual the grinding balls were 1/8 inch stainless steel balls, the fluid medium was toluene and the pedal was rotated at 500 rpm. After the grinding, the powder was removed from the chamber, dried and powder size was examined. Particle size distribution is shown in the micrograph in Figure 7 which is similar to the powder produced in the conventional setup. It appears that powder comminution in the chamber for low oxygen content would proceed satisfactorily.

ORIGINAL PAGE  
BLACK AND WHITE PHOTOGRAPH



TSA 2250

→ | | ← 20  $\mu$  m

Figure 7. Photomicrograph of the  $\text{SmCo}_5$  powder prepared by attritor ball milling in the comminution chamber.

## 7.2 Arc Welding Inside the Chamber

The success of the entire process would heavily depend on being able to produce a leak-tight welded joint between the cover and the cannister of the HIP assembly inside the chamber. Therefore, it was important to determine if welding could be successfully performed inside the chamber.

The chamber was evacuated to  $10^{-6}$  torr pressure and backfilled with high purity argon. Two 1/16 inch low carbon steel plates were then seam welded in several 4 inch lengths, providing manual movement of the gun using gloves. Since it was done in a 100 percent argon atmosphere, the welding electrode was not covered with flowing argon around it. There were some doubts about whether the welded joint could be made without an envelope of argon gas flowing around the electrode during the welding. The steel plates were brought out and visually examined for flaws. They were found to be of excellent quality, and were at least as good as similar welded joints produced when done in the conventional manner in room atmosphere.

## 7.3 SmCo<sub>5</sub> Powder Densification Using Commiution Chamber Procedure

Since there was little time left to carry on the many experiments necessary to show the dependence of coercivity on oxygen content, it was decided that at least some densification of SmCo<sub>5</sub> powder handled inside the chamber should be performed, which would of course be only of a preliminary nature. It was expected that this would indicate whether the procedures are viable, and whether they would indeed lead to production of fine-grained densified SmCo<sub>5</sub> bodies with significantly reduced oxygen content. The most reasonable approach would have been to first develop commiution procedures and drying of powder-toluene slurry in the commiution chamber in purified argon atmosphere maintaining very low levels of oxygen content. This alone would have taken more time

than we had left. Therefore, we decided to proceed with powders of much larger particle size, that could be produced by either disc pulverizer or hydrogen comminution. Hydrogen comminuted powder appeared attractive, since it could be produced without exposure to air and transferred to the chamber where the pressure vessel could be opened in the highly purified argon atmosphere, and perhaps would contain less oxygen than disc-ground powder.

A 100-gram batch of commercial  $\text{SmCo}_5$  alloy in half-inch size pieces was hydrogen comminuted with apparatus shown in Figure 6. The pressure vessel was first evacuated to  $10^{-6}$  torr, and then filled with hydrogen at 800 lb/in<sup>2</sup> for about 16 hours. Hydrogen was then removed by evacuation while the pressure vessel was heated to about 100°C by means of heating tapes. When the pressure reached low  $10^{-6}$  torr region, heating tapes were removed, the vessel was backfilled to 17 lb/in<sup>2</sup> with high purity tank argon, valved off from the system, disconnected at the o-ring seal joint and the vessel transferred to the chamber. The comminution chamber was evacuated to  $2 \times 10^{-6}$  torr and backfilled to slightly above atmospheric pressure with getter-furnace purified argon. Next, the pressure vessel cover was removed, and the following tasks were performed:

- (a) About 0.5 gm powder samples were placed inside preweighed tin capsules, which were pinched close and placed inside glass vials and tightly capped.
- (b) Powder was loaded under a pressure of 2000 pounds into two outgassed HIP cannisters, 3/4 inch internal diameter by 1-3/4 inch high, and 1/16 inch wall.
- (c) The outgassed assemblies of HIP can cover and pump-out tube swagelock connected to high vacuum valves were then welded to the cannisters, following which the valves were tightly shut. A welded HIP assembly is shown in Figure 8.



ORIGINAL PAGE  
BLACK AND WHITE PHOTOGRAPH

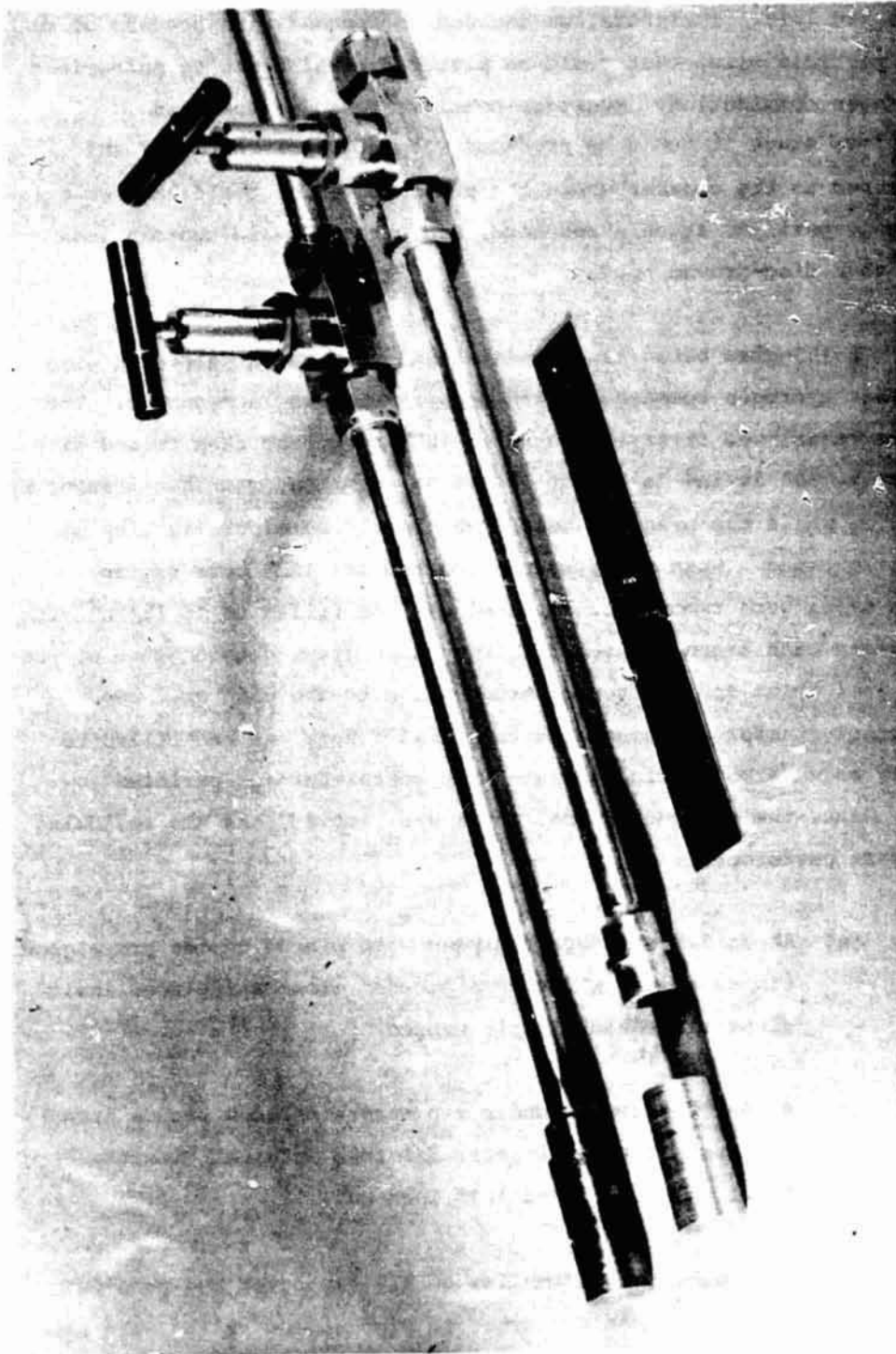


Figure 8. Welded and unwelded HIP cannisters and  
cover - valve assemblies.

TSA 2251

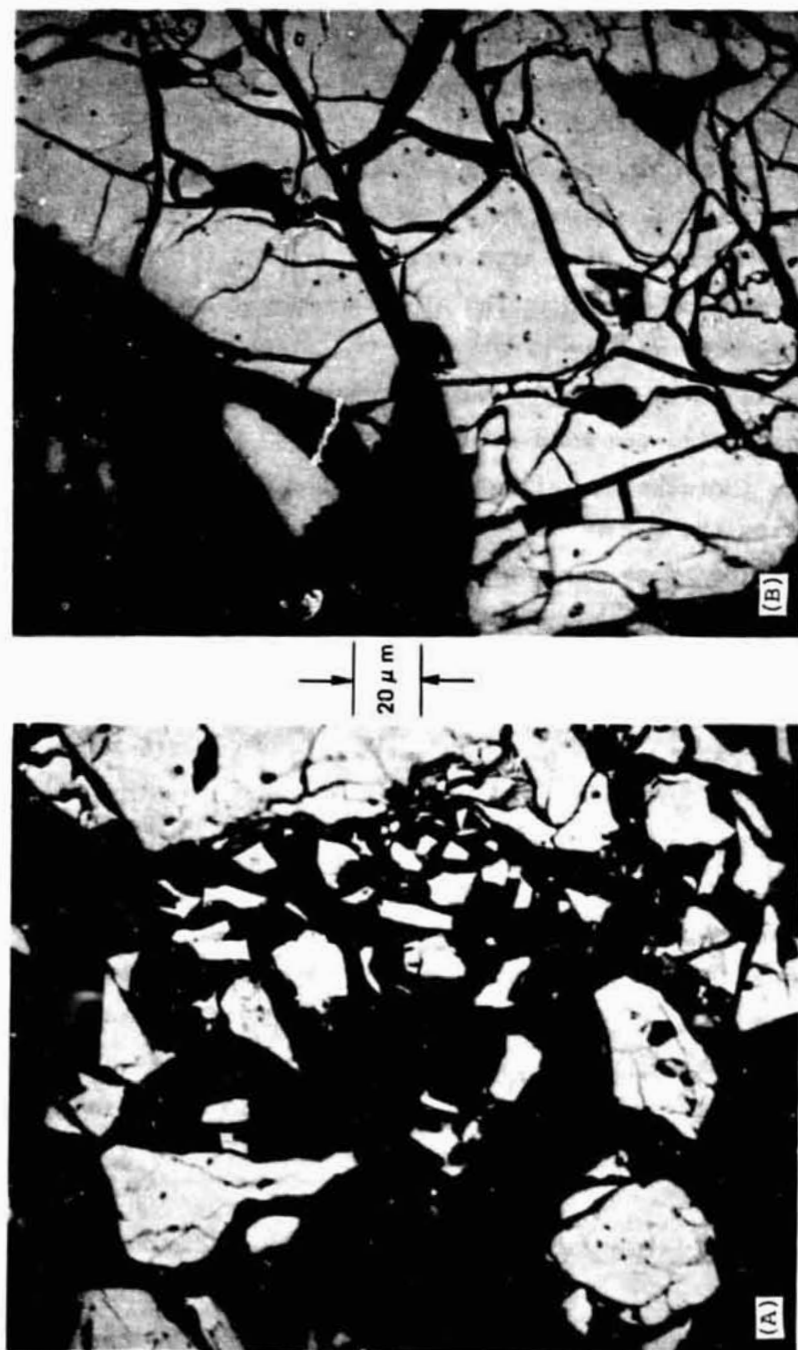
The HIP cannister assemblies, and the tin capsules were then removed from the chamber. A similar run was then made with 100 grams of high purity  $\text{SmCo}_5$  alloy purchased from the Ames Laboratory of Iowa State University. The powder samples in tin capsules were sent out to an outside laboratory for oxygen analysis. After attaching additional lengths of tubing to the valves by swagelock, the HIP cannisters were leak-checked and refilled with high purity argon and sent out for HIPing to a local HIP service company. The HIP procedure consisted of evacuation, bake out, seal by pinching of the steel tubing, and HIP at  $950^\circ\text{C}$  for 2 hours at  $15 \text{ lb/in}^2$  pressure of argon. All four HIPed cans, two each of commercial and Ames alloys, were found to have collapsed sufficiently to indicate successful HIPing. The HIPed  $\text{SmCo}_5$  compacts were removed from the cannisters by dissolution of the steel cans in dilute nitric acid. They were then OD ground to  $1/2$  inch diameters and sliced to produced  $0.150$  inch thick slices. Individual slices from each of the HIPed ingots were given the following heat treatments:  $1000^\circ\text{C}$  - 19 hours,  $1120^\circ\text{C}$  - 3 hrs and  $1140^\circ\text{C}$  - 3 hours. Following the above homogenizing treatments each group was aged at  $900^\circ\text{C}$  for 6 hours and then quick cooled.

One set of samples in as HIPed condition were sent out for oxygen analysis. Magnetic measurements for  $4\pi\text{M-H}$  characteristics were carried out in a 140 kOe Bitter solenoid at the National Magnet Laboratory of MIT using flux integration technique. Samples were also examined metallographically in as-HIPed condition as well as after the various heat treatments to determine porosity, grain size, and the presence and identification of the second phase.

### 7.3.1 Metallographic Examination

The powder characteristics of the hydrogen comminuted powder are shown in Figures 9(a) and 9(b). Some very fine particles around  $1 \mu\text{m}$  were formed - Figure 9(a) - but the bulk of the powder consisted of very large particles, although severely cracked. Both the commercial alloy and the Ames alloy showed similar behavior. In spite of the

ORIGINAL PAGE  
BLACK AND WHITE PHOTOGRAPH



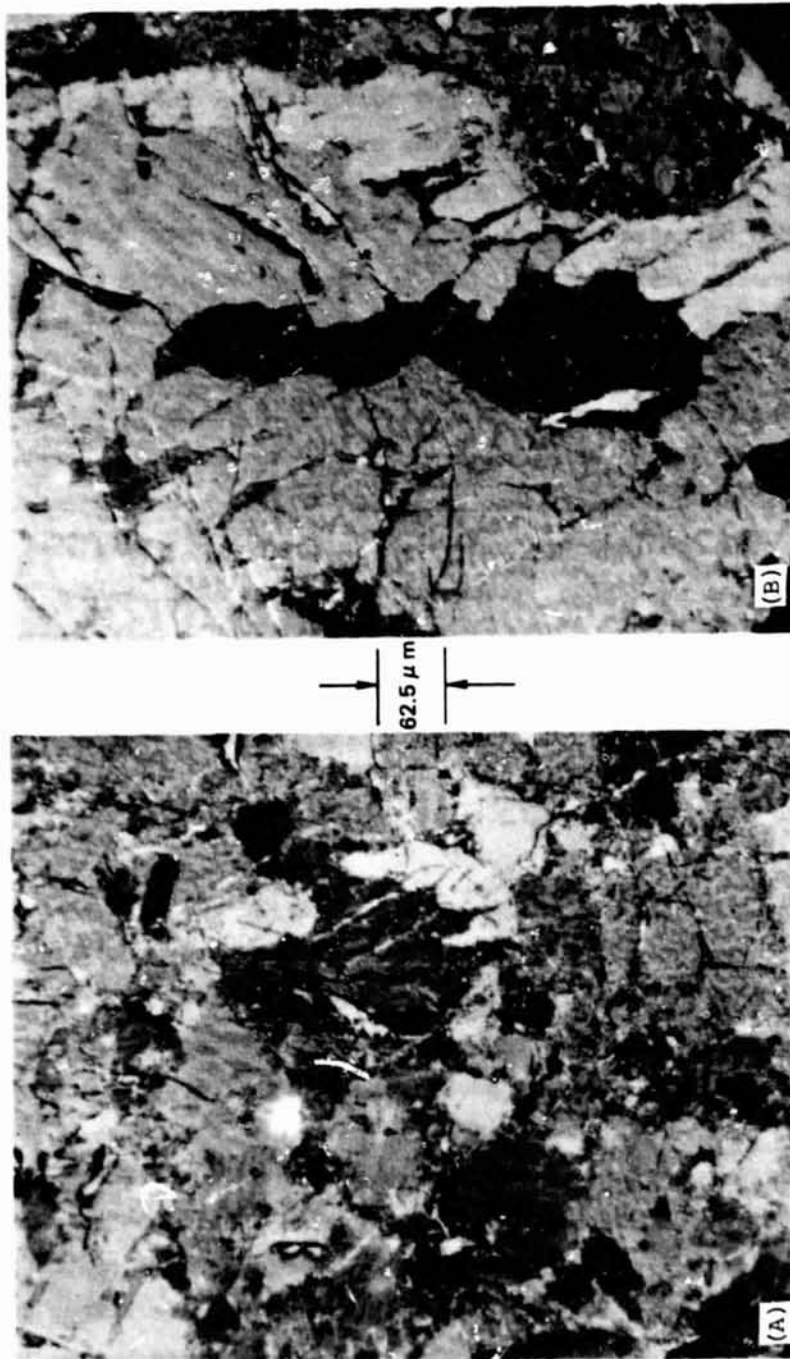
TSA 2252

Figure 9. Particle size of  $K_2$  comminuted  $SmCo_5$  powder. (A) Some fine particles.  
(B) Cracked large crystals, partially attached.

extremely large size of the particles the densification by HIP was quite satisfactory with the porosity close to 1 percent. The grain sizes of the HIPed samples are shown in Figures 10 and 11 for the commercial and Ames alloy. These microstructures were produced by cross-polarized light on as-polished HIPed samples, which not only show the magnetic domain patterns but also bring out the grain boundaries. There were some areas showing grains of 10 to 20  $\mu\text{m}$  size but such areas constituted less than 1 percent of the total. It was roughly estimated that 99 percent of the HIP densified body consisted of grains between 100 and 400  $\mu\text{m}$ . It appears that the large particles with cracks shown in Figure 9 rebonded along the cracks and became large single grains. The telltale traces of the cracks are still visible, with the magnetic domain boundaries freely going across them, which would make them behave as large particles in the demagnetization process. The smaller particles occupy such small volume that their magnetic contribution would be negligible. The coercivity of such a magnet material would be expected to be very low, in the neighborhood of zero, since it would be impossible to achieve required homogeneity in the large grains in real time.

Phase compositions of the  $\text{SmCo}_5$  densified bodies were determined by examination of the microstructure after etching the polished surfaces with 3 percent nital solution, which darkens the  $\text{Sm}_2\text{Co}_7$  particles causing them to show up in the light  $\text{SmCo}_5$  matrix. Figures 12 (a) and (b) show the phase compositions of the commercial alloy product in as-HIPed condition and after one of the heat treatments. Figures 13 (a) and (b) were corresponding structures of the Ames alloy product. The commercial alloy being about one-half weight percent richer in Samarium than the Ames alloy shows more of the Sm-rich  $\text{Sm}_2\text{Co}_7$  phase. For both alloys the as HIPed samples show larger amounts of  $\text{Sm}_2\text{Co}_7$  than after the heat treatment. This is caused by the larger composition homogeneity range of  $\text{SmCo}_5$  at the higher temperature. Second phase content shown by the HIPed samples would be quite adequate for production of high coercivity, if not hampered by other structural causes.

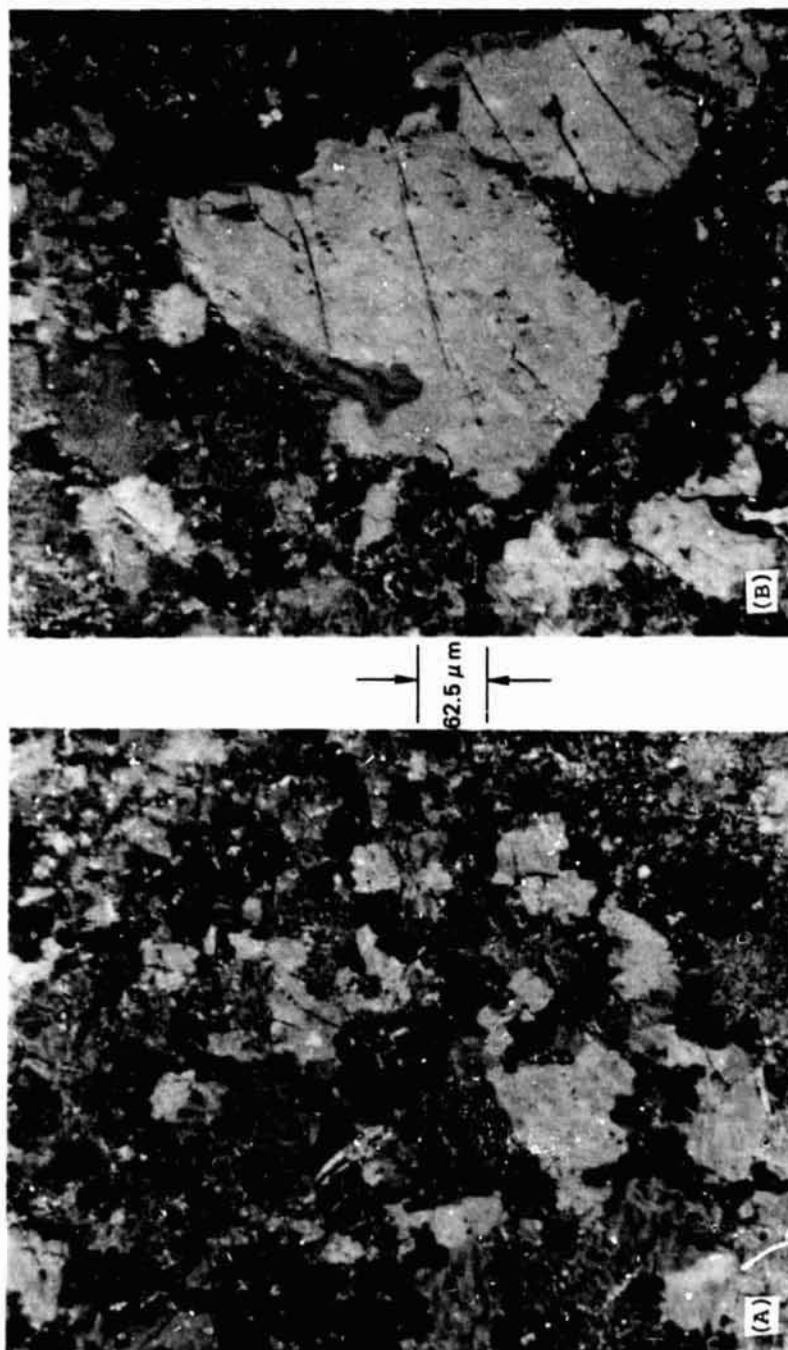
ORIGINAL PAGE  
BLACK AND WHITE PHOTOGRAPH



TSA 2253

Figure 10. Grain size and domain structure of polished HIP'd  $\text{SmCo}_5$  (commercial alloy)  
(A) Fine grain area. (B) Coarse grain area - predominant.

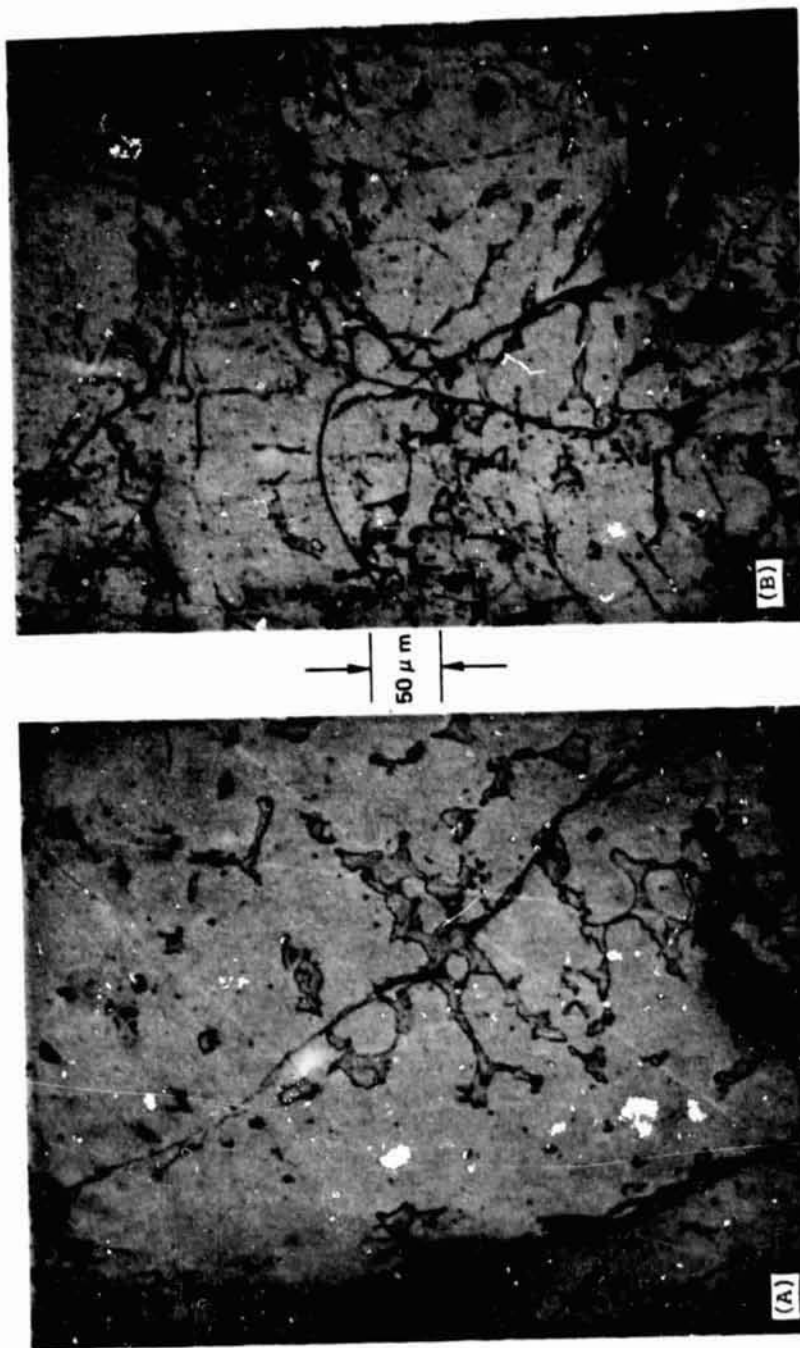
ORIGINAL PAGE  
BLACK AND WHITE PHOTOGRAPH



TSA 2264

Figure 11. Grain size and domain structure of polished HIP'd SmCo<sub>5</sub> (Ames alloy)  
(A) Fine grain area, (B) Coarse grain area - predominant.

ORIGINAL PAGE  
BLACK AND WHITE PHOTOGRAPH

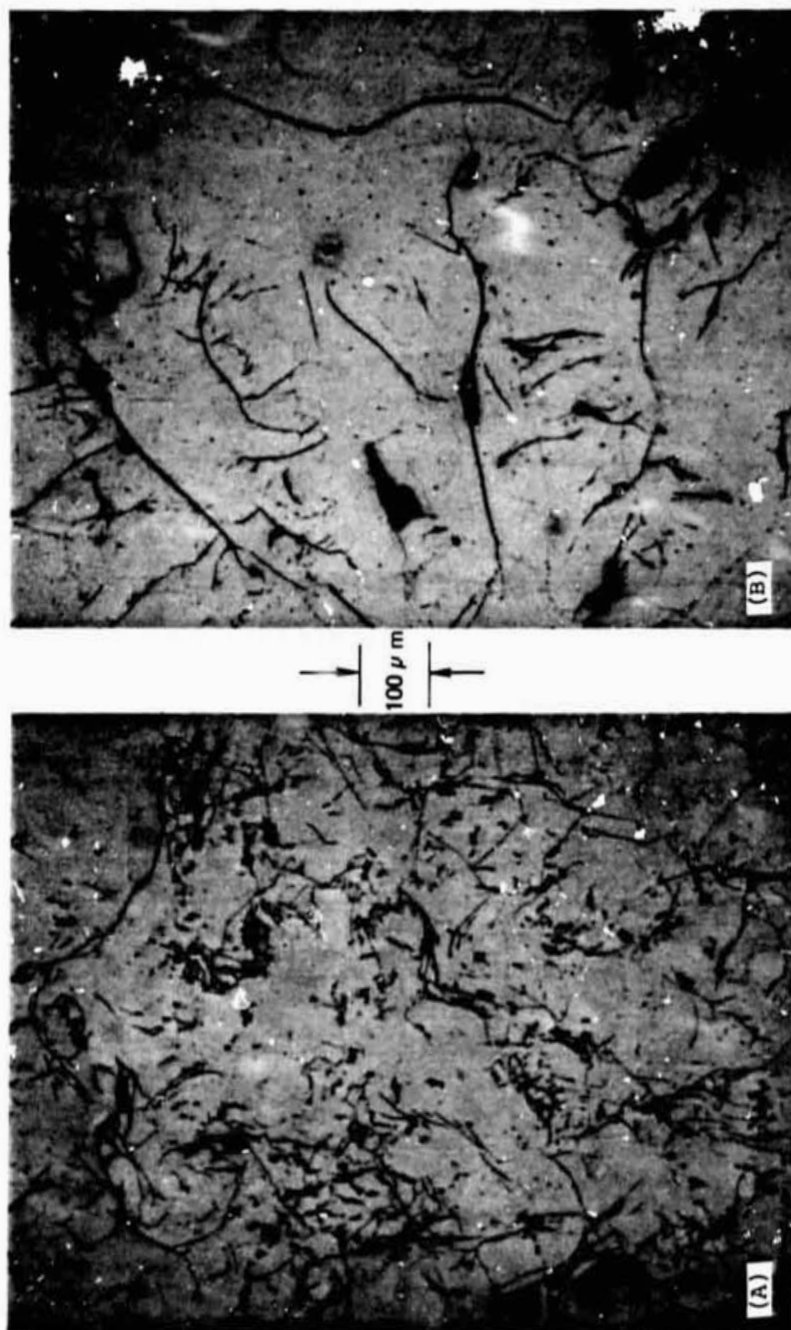


TSA 2255

Figure 12. Microstructure of commercial HIP'ed  $\text{SmCo}_5$ . Etched with 3% Nital to show dark grains of  $\text{Sm}_2\text{Co}_7$ . (A) As HIP'ed (B) Heat treated at  $1000^\circ\text{C}$ -19 hours  $\rightarrow$   $900^\circ\text{C}$ -6 hours, quick cooled.



ORIGINAL PAGE  
BLACK AND WHITE PHOTOGRAPH



TSA 2256

Figure 13. Microstructure of Ames Alloy HIP'ed  $\text{SmCo}_5$ . Etched to reveal  $\text{Sm}_2\text{Co}_7$  phase. (A) As HIP'ed  
(B) Heat treated at  $1000^\circ\text{C}$  - 19 hours  $\rightarrow$   $900^\circ\text{C}$  - 6 hours, quick cooled.



ORIGINAL PAGE IS  
OF POOR QUALITY.

### 7.3.2 Magnetic Properties

Although it was expected that the HIPed  $\text{SmCo}_5$  bodies with such large grain size would not possibly have coercivities very much above zero, measurements were made on these samples in the as-HIPed condition as well as after the three different heat treatments described earlier. These are shown in Table 2.

Table 2. Intrinsic coercivities of HIPed  $\text{SmCo}_5$  materials produced from  $\text{H}_2$ -comminuted powder.

Sample	Thermal History	Intrinsic Coercivity $H_{ci}$ - kOe
Commercial Alloy	As-HIPed	0
"	HIPed + 100°C - 19 hrs., 900°C - 6 hrs., Quick cooled	2.0
"	HIPed + 1120°C - 3 hrs., 900°C - 6 hrs., Quick cooled	2.0
"	HIPed + 1140°C - 3 hrs., 900°C - 6 hrs., Quick cooled	2.5
Ames Alloy	As HIPed	0
"	HIPed + 1000°C - 19 hrs., 900°C - 6 hrs., Quick Cooled	2.0
"	HIPed + 1120°C - 3 hrs., 900°C - 6 hrs., Quick Cooled	3.0
"	HIPed + 1140°C - 3 hrs., 900°C - 6 hrs., Quick Cooled	2.0

### 7.3.3 Oxygen Analyses

Oxygen analyses were performed on both the commercial and the Ames laboratory alloys, the hydrogen comminuted powders from these alloys, and the HIP densified bodies formed from these powders. The results of these analyses are shown in Table 3.

# CRUCIBLE WALLS OF POOR QUALITY

Table 3. Oxygen analyses of various samples.

Alloy	Condition	Oxygen Content ppm
Ames Laboratory	As-received	70
"	H <sub>2</sub> -comminuted powder	468
"	HIPed body of above powder	470
Commercial	As-received	130
"	H <sub>2</sub> -comminuted powder	1400
"	HIPed body of above powder	640

## 8. DISCUSSION AND CONCLUSIONS

The objective of the present program was to approach the theoretical maximum coercivity in SmCo<sub>5</sub> magnets. This was to be accomplished by reducing oxygen contamination that results when the powder metallurgical process used for fabricating these magnets is carried out in ordinary air atmosphere as in the conventional state-of-the-art commercial processing. The theoretical maximum value of coercivity is about 350 kOe. The best value of coercivity in SmCo<sub>5</sub> magnets produced by powder metallurgical process having grain size between 10 and 20  $\mu$ m is around 45 kOe. These magnets contain a minimum of about 6000 ppm of oxygen. Arc plasma sprayed SmCo<sub>5</sub> magnets produced at the C.S. Draper Laboratory with grain size of less than 5  $\mu$ m and oxygen content in the range of 1500 to 2000 ppm have, however, showed coercivity values close to 70 kOe. It was, therefore, expected that if the oxygen content could be further reduced while maintaining a very small grain size the coercivity would increase above what has been achieved for the sprayed magnets. In addition to the oxygen contamination, the commercially prepared SmCo<sub>5</sub> alloys contain various other impurities, a large fraction of which comes from the crucible walls in which the alloys are melted. Based on the above rationale, this program was initiated to produce very fine-grained SmCo<sub>5</sub> magnets

with the lowest possible oxygen content and lowest possible content of the other impurities. The two main tasks for the program were to (1) produce a high purity  $\text{SmCo}_5$  alloy with oxygen content as low as possible and (2) develop processes for powder preparation, cold compaction and densification which would avoid further oxygen contamination.

Two approaches taken for the alloy melting procedure were R.F. levitation melting in flowing helium and D.C. arc melting on a water-cooled tantalum-clad copper hearth in a purified quiescent argon atmosphere. Both the methods avoided contamination caused by reaction with crucible walls. As compared to an oxygen content of about 150 ppm in commercial alloys, when carefully controlled, the D.C. arc melted alloy gave an oxygen analysis of 70 ppm and the R.F. levitation melted alloy showed 200 ppm. The higher oxygen content of the levitation melted alloy is believed to have come from the high velocity helium gas jet used for controlling the temperature of the melt. Therefore, it is reasonable to expect that the oxygen content of a similar alloy melted in zero gravity, where no cooling gas jet would be required, will be similar to the D.C. arc melted alloy, or lower.

The second task, viz the fabrication of densified fine powder magnet from the alloy, has not been completed at the conclusion of this program because of the untimely termination of the activity. Considerable effort has gone into this task and some encouraging results have been obtained in avoidance of oxygen contamination, as discussed in detail below.

As already mentioned, a good quality commercial alloy may contain as little as 150 ppm of oxygen. An increase of oxygen content by a factor of 40, to 6000 ppm, occurs during the fabrication process. Practically all of it occurs during the preparation of the powder and its subsequent handling in the air atmosphere. For this task a special chamber was built which provided an oxygen-free, inert gas atmosphere for carrying out powder preparation, compaction of the powder, and encapsulation of the compact inside a welded outgassed HIP cannister.

The chamber, which has been built of stainless steel with polished walls and stainless steel plumbing, is capable of being evacuated and baked out to reach a low  $10^{-6}$  torr pressure. Besides the main chamber where all the powder preparation and handling, etc. are performed using gloves, there are two attached auxiliary chambers, one for powder drying and the other an entry port, each of which can be individually evacuated or filled with purified gas. The chamber can be backfilled with getter furnace purified argon gas. Powder comminution, compaction and welding of HIP cannisters are performed in the main chamber, with rotary motion and electrical powder brought in by special feedthroughs.

By the time the chamber was installed, all the necessary accessories built and incorporated into the chamber, and various functions to be performed tested, the time necessary to develop the procedures for oxygen-free fine powder production was not available.

The experiments carried out for fabrication of densified  $\text{SmCo}_5$  powder bodies using the newly built comminution and encapsulation chamber, though limited in scope, have nonetheless yielded encouraging results on avoidance of oxygen contamination that invariably occurs in the conventional processing. The oxygen pickup in the final densified bodies from the time the powder entered the chamber through the many steps of processing involved, was near zero. The excessively high oxygen content shown by the commercial alloy powder was possibly caused by a leak in the tin capsule in which it was contained.

The choice of performing the experiments with hydrogen comminuted powder, as it turned out, was an unfortunate one. Not only did it give an unexpectedly high oxygen contamination of at least 500 ppm, but also produced the very large grain size of 400  $\mu\text{m}$  in the HIPed material. A better choice for the powder would have been the regular disc ground powder after rejecting the -100 mesh fraction of the powder by sieving. The powder particle size in such a powder would have been only 100 to 150  $\mu\text{m}$  and an oxygen contamination, solely due to disc grinding, would not have exceeded 150 ppm.

The coercivities of the first batch of HIPed samples prepared in the clean chamber were expected (and measured) to be near zero, because of the very large grain size seen on microexamination. The primary requirements for high coercivity in  $\text{SmCo}_5$  magnets are correct chemical composition, low impurity (particularly oxygen), and small grain size which facilitates homogenization. The composition should be such that the samarium content is slightly in excess of the  $\text{SmCo}_5$  stoichiometry, but never less than the stoichiometry. The most desirable grain size in the finished magnet should be less than 5  $\mu\text{m}$ . Although the composition and purity requirements were met in our initial experiments, the grain size requirement was missed by an overwhelming margin.

Because of the considerable success that was achieved in eliminating oxygen contamination during fabrication of the densified powder body, further work will now be continued as part of an existing related program. The funding support for this work will come from our on-going ONR funded program on developing Rare Earth-Cobalt magnets for advanced inertial applications.

#### LIST OF REFERENCES

- (1) Das, K., K. Kumar, E. Wettstein, Materials Research for Advanced Inertial Instrumentation, Task 3, Rare Earth Magnetic Materials Technology, The Charles Stark Draper Laboratory, Inc., Cambridge, MA 02139, Report No.2, October 1979.
- (2) Kumar, K., D. Das, E. Wettstein, "High Coercivity Isotropic Plasma Sprayed Samarium-Cobalt Magnets," J. Appl. Phys., 49, p 2050, 1978.
- (3) Livingston, J.D., "Present Understanding of Coercivity in Cobalt Rare Earth Magnets," AIP Conference Proceedings MMM (1972).
- (4) Bartlett, R.W., and P.J. Jorgensen, "Microstructural Changes in  $\text{SmCo}_5$  Caused by Oxygen Sinter-Annealing and Thermal Aging," J. Less Common Metals, 37, p 21, (1974).
- (5) Das, D., and W. Harrold, "Characterization of Samarium-Cobalt TWT Magnets," IEEE Trans. Magnetics, MAG-7, No. 2, p 281, June 1971.
- (6) Kumar, K., D. Das, and E. Wettstein, IEEE Trans. Magnetics, Vol. Mag 14, No. 5, p 788 (1978).
- (7) Das, D., K. Kumar, "Hot Isostatically Pressed  $\text{SmCo}_5$  Magnets" IEEE Trans. Magnetics, MAG-16, No. 5, p 1000, Sept. 1980.
- (8) Chang, C.W., D.K. Das, R.T. Frost, and K. Kumar, "Electromagnetic Containerless Reaction of Samarium with Cobalt for the Formation of Samarium-Cobalt Alloys," Metallurgical Transactions, October 1982.

APPENDIX 1  
ELECTROMAGNETIC CONTAINERLESS REACTION OF  
SAMARIUM WITH COBALT FOR THE  
FORMATION OF SAMARIUM-COBALT ALLOYS

C. W. Chang\*, D. K. Das\*\*, R. T. Frost\* and K. Kumar\*\*

\* General Electric Company, Space Systems Division, P.O. Box 8555,  
Philadelphia, PA 19101.

\*\* The Charles Stark Draper Laboratory, Inc., 555 Technology Square,  
Cambridge, MA 02138

PRECEDING PAGE BLANK NOT FILMED

Magnetization reversal in  $\text{SmCo}_5$  magnets has been found to result from nucleation and motion of reverse magnetic domains. This is believed to be associated with the presence of defect sites in the conventionally prepared  $\text{SmCo}_5$  magnets. Work at the Charles Stark Draper Laboratory and elsewhere<sup>(1,2,3)</sup> indicates that these defects may be compositional inhomogeneities resulting from precipitation of dissolved oxygen during cooling of the magnet from sintering and optimization temperatures. Because of the high chemical reactivity of the samarium, other contaminants also enter the alloy from the crucible materials in which the  $\text{SmCo}_5$  alloys are formed. These other contaminants are also suspected to be contributors to undesirable defects.

Ideally, crucible contamination can be eliminated completely by the reaction of the pure elements while levitated by electromagnetic fields. There is a noticeable absence of papers that report detailed studies of formation of an alloy from solid materials by levitation technique except the work by Polonis et al.<sup>(4)</sup>. The work reported here describes the successful application of this technique to formation of near stoichiometric  $\text{SmCo}_5$  by suitable formation of charges of the elemental materials and by use of a gas jet to control temperature during the reaction. Although temperature control was rendered difficult by the requirement of field intensities capable of levitating the specimen against gravity, sufficient control was obtained to allow achievement of stoichiometry approximating  $\text{SmCo}_5$  composition by providing excess Sm in the charge to compensate for evaporation during temperature excursions.

The General Electric levitation facility<sup>(5)</sup> (450 kHz, 25 kw RF power generator) was used for carrying out the reaction experiments. Elemental samarium from Cotronics Corp. and United Mineral and Chemical Corp. and cobalt from Materials Research Corp. were obtained for the experiments. A radiation pyrometer was assembled by using optical filters (0.65 and 0.85 microns) and a CID (Charge Injection Device) imager. Pyrometer calibration is mandatory to provide accurate



temperature readings. Observation of melting of gold (m.p. 1336°K) and Constantan's (m.p. 1543°K) wires inserted into small cavities drilled into cobalt specimens was used for absolute calibration. The developed instrumentation was employed as described later for controlling reaction temperatures for compacts of elemental samarium and cobalt where a containing cobalt jacket was used, at least up to the point where the outer surface of the capsule participated in the reaction.

A gas injection device was installed for cooling the levitated melt. Also, a helium scrubber was constructed and placed in operation which is capable of removing the major part of the oxygen and water vapor contaminant by passing the gas sequentially through a liquid nitrogen trap and through copper screens heated to 600°C in an oven. In the experiments, helium gas played the major role in cooling and solidifying the levitated melt<sup>(5)</sup>. Gas velocities of the order of 30 meters per second or greater were required to achieve solidification.

A technique for the containerless reaction of elemental samarium and cobalt to form the alloy was next developed. Charges were fabricated consisting of a 1 cm diameter closed cylindric capsule of cobalt containing a tightly fitting cylinder of samarium, with volume adjusted to provide the desired ratio of elements in the alloy, corresponding to near-stoichiometric  $\text{SmCo}_5$ . Several reaction experiments at different reaction time and cooling rate were performed with immediate success. Figure 1 shows the exterior of a typical specimen after reaction experiment. The results of several experiments are listed in Table 1. Total weights of the specimens before and after experimentation are presented in Table 1. The weight losses of the specimens are assumed to be primarily samarium from calculations based on vapor pressure. The initial and final contents of samarium are also included in Table 1. By applying the reaction model described by levenspiel<sup>(6)</sup>, the reaction rate of samarium with cobalt for Specimen No. 1 was estimated to be in the order of  $1.0 \times 10^{-3}$  cm/sec around the temperature of 1300°C by using the approximate reaction time 84 sec from the test. The estimated result indicates that the reaction rate of

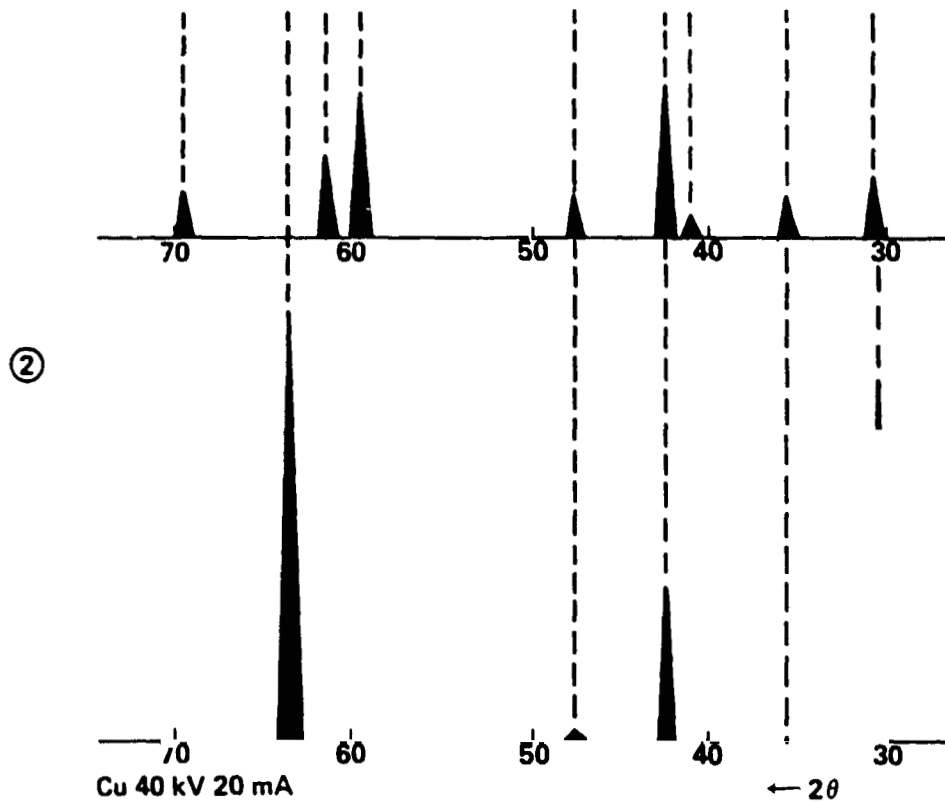
ORIGINAL PAGE IS  
OF POOR QUALITY.



Figure 1. The appearance of a typical melt of Sm-Co alloy by R.F. Levitation.

ORIGINAL FILED  
OF POOR QUALITY.

① 'd' → 1.356 1.464 1.513 1.556      1.901 2.116 2.180 2.498 2.929  
 Int → 14 10 10 11      5 100 50 36 60  
 hkl → (301) (202) (211) (112)      (201) (111) (021) (110) (111)

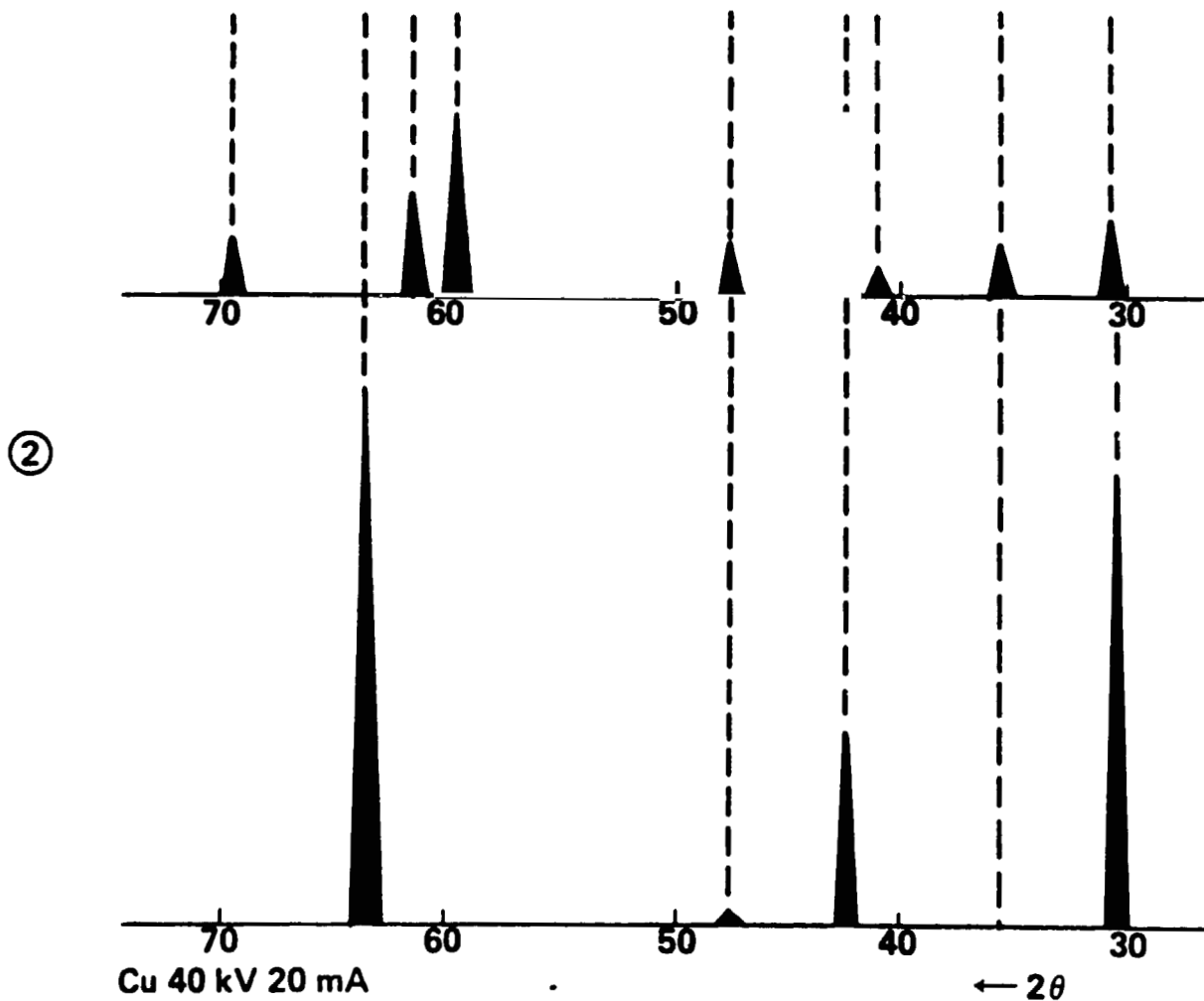


10/80 CD21684  
 REV A 1/82

Figure 2. X-ray diffraction patterns of samples No. 1 and 2.

ORIGINAL PAGE IS  
OF POOR QUALITY

① 'd' → 1.356 1.464 1.513 1.556      1.901 2.116 2.180 2.498 2.929  
Int → 14 10 10 11      5 100 50 36 60  
hkl → (301) (202) (211) (112)      (201) (111) (021) (110) (111)



10/80 CD21664  
REV A 1/82

Figure 2. X-ray diffraction patterns of samples No. 1 and 2.

samarium with cobalt is much larger than the diffusion rate between liquid samarium and solid cobalt.

Specimens after reaction experiments were further evaluated to determine compound formation, uniformity of composition and amount of oxygen pickup. Elemental samarium and cobalt used for preparing alloys and the obtained alloy, were analyzed for oxygen content using inert gas fusion technique. The results are given in Table 2.

X-ray diffractometer patterns were obtained from the longitudinally sectioned plane of the melted ingots. Two such patterns are shown in Figure 2. Also, optical micrographs of samples No. 1 and 2 are shown in Figure 3. By inspecting the X-ray diffractometer patterns as shown in Figure 2, every line in all the patterns can be accounted for by the diffraction pattern of the compound  $\text{SmCo}_5$ . The peak intensities of the lines showed no correspondence to those obtainable from a powder pattern of  $\text{SmCo}_5$ . This is believed to be caused by the large size of grains, which resulted in only a few grains accommodated in the X-ray beam, and not as a result of any preferred orientation of crystallites during solidification.

Since the compositions of both the alloys were richer in Sm than the stoichiometric  $\text{SmCo}_5$  (33.8% Sm), they were expected to contain small amounts of  $\text{Sm}_2\text{Co}_7$ . Although no  $\text{Sm}_2\text{Co}_7$  peaks were seen in the X-ray diffraction patterns, optical microstructures (Figures 3a and 3c) showed well distributed  $\text{Sm}_2\text{Co}_7$  phase throughout the ingots except for the very tips. The tips constituted less than 0.1 percent of the total volume. SEM-EDAX scans verified that the matrix throughout had the  $\text{SmCo}_5$  composition including the tip area and that the second phase (dark grains) were  $\text{Sm}_2\text{Co}_7$ .

Kerr-effect magnetic domain patterns were obtained by the use of cross polarized light beam microscopy. The magnetic domain patterns corresponding to Figures 3a and 3c are shown in Figures 3b and 3d, respectively. Individual grains are seen to be clearly delineated

ORIGINAL PAGE IS  
OF POOR QUALITY

Table I. Weight Analysis of Specimens Before and After Reaction

<u>Specimen No.</u>	<u>Weight, g</u> <u>(Before)</u>	<u>pct Sm</u> <u>(Before)</u>	<u>Weight, g</u> <u>(After)</u>	<u>pct Sm</u> <u>(After)</u>
1	6.1989	34.65	6.1378	34.00
2	6.1353	35.64	6.0046	34.29
3	4.8595	36.78	4.7734	35.63
4	4.8567	36.79	4.6864	34.49

Table II. Oxygen Content Analysis

<u>Specimen No.</u>	<u>Sm</u> <u>ppm</u>	<u>Co</u> <u>ppm</u>	<u>Sm-Co Alloy</u> <u>ppm</u>
1	120	<100	560
2	120	<100	580
3	1	27	200
4	1	27	400

because of different degrees of shading as well as differences in domain structures. The grains are quite large and in millimeter range, and crystallographically they are of random orientation.

The substantial increase in the oxygen content of the alloys over that of the starting metals must have been acquired from the helium jet used for controlling the temperature of the levitated melt. We feel that the chemical composition, crystalline structure, and the uniformity of the phase distribution as seen in the levitated melt would be satisfactory for our research studies on magnetic properties. The oxygen content, however, was too high and efforts should be made to lower it by an order of magnitude in a future study.

The homogeneity of resultant alloys was verified on the basis of X-ray diffraction and SEM-EDAX analysis. In contrast to the poor mixing reported by El-Kaddah and Robertson<sup>(7)</sup>, the result of this study shows that substantial stirring exists in a RF levitated melt. This fact indicated an additional advantage for forming highly reactive materials by the electromagnetic levitation method.

This program was supported under the NASA Materials Processing in Space Program by the George C. Marshall Space Flight Center. Development of the elemental samarium and cobalt charge forming technique, as well as new procedures in operation and control of the levitation system, were contributed by Daniel J. Rutecki.

ORIGINAL PAGE  
BLACK AND WHITE PHOTOGRAPH



Figure 1. Typical bright field and Kerr-effect micrographs of 3% NITAL-etched levitation melted Sm-Co alloys. (a) Sample #1 - Bright field; (b) Kerr-effect image of same area as in (a); (c) Sample #2 - bright field; (d) Kerr-effect image of same area as in (c).



### References

1. R. W. Bartlett and P. J. Jorgensen: J. Less Common Metals, 1974, Vol. 37, p. 21.
2. D. Das and W. Harrold: IEEE Trans. Magnetics, 1971, MAG-7, p. 281.
3. K. Kumar, D. Das and E. Wettstein: IEEE Trans. Magnetics, 1978, MAG-14, p. 788.
4. D. H. Polonis, R. G. Butters and J. Gordon Parr: Resesarch, 1954, vol. 7, p. 273.
5. G. Wouch, E. C. Okress, R. T. Frost and D. J. Rutecki: Rev. Sci. Inst., 1975, vol. 46, p. 1122.
6. O. Levenspiel: Chemical Reaction Engineering, p. 338, John Wiley & Sons, Inc., New York, 1962.
7. N. H. El-Kaddah and D. G. C. Robertson: Met. Trans. B, 1978, vol. 9B, p. 191.